

AMERICAN UNIVERSITY OF BEIRUT

PLASMA KALLIKREIN AS A NOVEL MODULATOR OF
MACROPHAGE DYNAMICS

by
MARYAM MOHSEN BEYDOUN

A thesis
submitted in partial fulfillment of the requirements
for the degree of Master of Science
to the Department of Biochemistry and Molecular Genetics
of the Faculty of Medicine
at the American University of Beirut

Beirut, Lebanon
March 2020

AMERICAN UNIVERSITY OF BEIRUT

PLASMA KALLIKREIN AS A NOVEL MODULATOR OF MACROPHAGE DYNAMICS

by
MARYAM BEYDOUN

Approved by:

Dr. Ayad Jaffa, Professor
Department of Biochemistry and Molecular Genetics.



Advisor

Dr. Aida Habib, Professor
Department of Biochemistry and Molecular Genetics




Member of Committee

Dr. Firas Kobaissy, Associate professor
Department of Biochemistry and Molecular Genetics



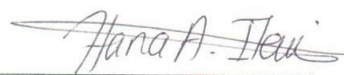
Member of Committee

Dr. Pierre Khoueiry, Assistant professor
Department of Biochemistry and Molecular Genetics



Member of Committee

Dr. Hana Itani, Assistant professor
Department of Pharmacology and Toxicology



Member of Committee

Date of thesis defense: March 12, 2020

AMERICAN UNIVERSITY OF BEIRUT

THESIS, DISSERTATION, PROJECT RELEASE FORM

Student Name:

MOHSEN BEYDOUN MARYAM
Middle Last First

Master's Thesis Master's Project Doctoral Dissertation

I authorize the American University of Beirut to: (a) reproduce hard or electronic copies of my thesis, dissertation, or project; (b) include such copies in the archives and digital repositories of the University; and (c) make freely available such copies to third parties for research or educational purposes.

I authorize the American University of Beirut, to: (a) reproduce hard or electronic copies of it; (b) include such copies in the archives and digital repositories of the University; and (c) make freely available such copies to third parties for research or educational purposes after:

One --- year from the date of submission of my thesis, dissertation, or project.
Two --- years from the date of submission of my thesis, dissertation, or project.
Three ~~---~~ years from the date of submission of my thesis, dissertation, or project.

~~Maryam~~ 01/06/20
Signature Date

This form is signed when submitting the thesis, dissertation, or project to the University Libraries

ACKNOWLEDGEMENTS

In the Name of Allah, the Most Beneficent, the Most Merciful.

First and most importantly, I would like to thank Allah (swt) for all the blessings He has bestowed upon me, without his guidance I wouldn't be where I am today.

It is with immense gratitude that I acknowledge the support and help of my professor and thesis advisor, Dr. Ayad Jaffa, for his direction, constant supervision as well as encouragement in helping me become the independent scientist I am today.

I'm highly indebted to Dr. Aida Habib for her constant assistance and advice; whether the subject matter was academic or not. I would also like to thank Dr. Pierre Khoueiry for teaching me all there is to know about Bioinformatics and Dr. Firas Kobeissy for his guidance throughout this thesis. My sincere thanks also goes to Dr. Hana Itani for being on my thesis committee, it is of great pleasure to me.

I thank my fellow lab-mates: Dr. Wared Nouredine for teaching me the laboratory techniques that I have performed in the frame of my thesis work as well as Batoul Maatouk, Mia Karam and Duaa Fahs for making the journey a fruitful and wonderful one and helping me whenever I was in need. You guys have formed the core of my research time.

I would like to express my gratitude to my friends Dr. Layla Kamareddine for her continuous guidance, Zeinab Hamzé for her constant encouragement and providing me with the friendship that I needed and Zahra Zreik for being an overwhelmingly essential part of my life.

I would like to thank Mohammad El-Harakeh in particular, for being a true and great supporter and always willing to help. I could not imagine my journey without you.

A very special word of thanks goes to Abbas Bazzi who has given me the extra strength and motivation to reach where I am today.

Finally, nobody has been more important to me in the pursuit of this project than the members of my family. I would like to dedicate this thesis to my mother and sisters who have given me the opportunity of an education from the best institutions and support throughout my life. I love you all very much!

AN ABSTRACT OF THE THESIS OF

Maryam Mohsen Beydoun for Master of Science
Major: Biochemistry and Biomedical Sciences

Title: Plasma Kallikrein as a Novel Modulator of Macrophage Dynamics

Introduction: Cardiovascular diseases (CVD) remain the leading cause of death globally, by which more than 17 million individuals die each year, accounting for 30% of all deaths. Moreover, CVD is responsible for 34% of all deaths in the Middle East, whereby the rate of increase in CVD-associated mortalities is one of the highest rates worldwide. Earlier studies have shown that elevated levels of plasma kallikrein is implicated in the perpetuation of CVD. In the cardiovascular system, plasma kallikrein is a key regulator of several proteolytic cascades. One of these cascades includes the kallikrein-kinin system (KKS). Therefore, it has been proposed that several components of the KKS are mediators or modulators of inflammation and that plasma kallikrein in specific plays an essential role in inflammation. Being a vital component of inflammation, monocytes are mobilized to the heart where they differentiate into macrophages. Following MI, monocyte-derived macrophages are able to secrete a wide range of factors that contribute to several processes such as inflammation, angiogenesis, repair system and phagocytosis. Since the plasma kallikrein-mediated inflammatory processes remain ill-defined and are poorly understood, this project seeks to characterize and assess the inflammatory markers involved in the macrophage-regulated pathogenesis of CVD.

Methods: To achieve these goals, we employed bone marrow-derived macrophages (BMDM) from C57BL/6 mice. Accordingly, we first cultured the aforementioned cells and treated them with plasma kallikrein for twenty-four hours. Lipopolysaccharide (LPS), a component of the gram-negative bacterial cell wall that is known as a pro-inflammatory factor, was used as a positive control in our study. In order to quantify the level of markers at the protein level, Enzyme-Linked Immunosorbent Assay (*ELISA*) was performed. To further demonstrate the expression of the markers at the transcript level, we extracted RNA from the cells and conducted Next Generation Sequencing (NGS) so as to elucidate gene expression signatures as well as compare and contrast the transcriptome of the treated and untreated BMDM using RNA-sequencing (RNA-seq). This was done in order to demarcate differentially expressed genes and profiles in the course of plasma kallikrein- and bradykinin-mediated inflammatory processes using specific bioinformatics tools. Genes that were differentially expressed, were identified and their expression profiles were

validated by Quantitative Reverse Transcription (RT-qPCR). In addition, we studied the biological network of proteins using Pathway Studio software in order to understand the processes involved in inflammation and CVD. Finally, to identify the receptors in plasma kallikrein-mediated inflammatory responses, the secretion of inflammatory cytokines was investigated after-which receptors were inhibited.

Results: Preliminary analysis pointed out the upregulation of pro-inflammatory cytokines in BMDM, of which include Tumor Necrosis Factor-Alpha (TNF- α) and Interleukin-6 (IL-6). The following results were observed at the protein level using *ELISA*. Moreover, RNA-seq data have also demonstrated the up and down-regulation of several inflammatory and fibrotic markers, which were further validated using RT-qPCR.

Conclusion: In this project, we expect to find novel mechanisms underlying the plasma kallikrein mediated inflammatory pathway, through monocyte-derived macrophages. Likewise, this project will serve to expand our current limited knowledge on the role of plasma kallikrein during inflammation in CVD and delineate the interplay between multiple factors, hence paving the way to the development of new therapeutic targets.

CONTENTS

ACKNOWLEDGEMENTS	v
ABSTRACT	vi
ILLUSTRATIONS	xi
TABLES	xiii
Chapter	
I. INTRODUCTION.....	1
A. Inflammation	1
1. Overview	1
2. Immune Cells in Inflammation.....	3
3. Macrophages.....	3
a. Origin, Role and Tissue Distribution	Error! Bookmark not defined.
b. Phenotypes.....	5
B. Cardiovascular Diseases.....	9
1. Overview	9
a. Epidemiology.....	11
b. Pathology.....	12
c. Integration of Macrophages.....	14
d. Prognosis	16
e. Therapies	16
C. Kallikrein-Kinin System	17
1. Plasma Kallikrein: Synthesis, Structure and Function.....	18
2. Receptors.....	19
a. Bradykinin Receptors (BKR).....	19
b. Protease-Activated Receptors (PARs)	20
II. MATERIALS AND METHODS	25

A. Bone Marrow-Derived Macrophages	25
1. Isolation and Culture.....	25
2. Splitting and Plating.....	26
3. Treatment	27
B. Stimulation	27
1. Treatment Concentration.....	27
2. Receptor Antagonists Concentration	27
C. Total RNA Extraction	28
D. Whole Transcriptome Sequencing Analysis	29
E. Pathway Analysis	31
F. Two-step Reverse Transcription Quantitative Polymerase Chain Reaction (RT-qPCR)	
.....	31
1. Reverse Transcription of RNA to cDNA	31
2. Quantitative Polymerase Chain Reaction (qPCR).....	33
G. Enzyme Linked Immunosorbent Assay (<i>ELISA</i>)	36
H. Statistical analyses	37
III. RESULTS	38
A. Differentiation of bone marrow-derived cells to macrophages.....	38
B. Inflammatory effect of BK- and PK-stimulated macrophages.....	39
C. Stringent RNA Quality Control using Bioanalyzer	41
D. RNA-seq Data Processing.....	44
E. Clustering of the Expressed Genes via Heatmap	48
F. Investigation of the Transcriptomic Data	50
G. Differential Gene Expression	51
H. Investigation of the Comparative Gene Expression via Venn Diagram.....	59
I. Identification of Altered Pathways.....	61
J. Validation of the Transcriptomic Data <i>via</i> RT-qPCR	67
K. Network Pathway Analysis of Transcriptomic Data	69
L. Investigation of Bradykinin and Protease-Activated Receptors Expression in Bone Marrow-Derived Macrophages	77
M. Identification of Receptors in PK-Mediated Inflammatory Response.....	78

IV. DISCUSSION.....	80
REFERENCES	84

ILLUSTRATIONS

Figure 1 Immune cell lineage.....	5
Figure 2 Activation markers and effectors of M1 macrophages.....	6
Figure 3 Activation markers and effectors of M2 macrophages.....	8
Figure 4 Anatomy of a heart attack.	10
Figure 5 Cleavage of kininogen into bradykinin.....	19
Figure 6 Protease activated receptors.	20
Figure 7 Representation of the process of isolating and culturing of BMDM from mice.	26
Figure 8 Experimental design of BMDM treated cells.....	27
Figure 9 RNA-Seq experimental workflow	30
Figure 10 Serial Dilutions of ELISA Standard	36
Figure 11 Bone marrow-derived cells.	38
Figure 12 Effect of Plasma Kallikrein and its mediator Bradykinin on Inflammatory Cytokines.....	40
Figure 13 Bioanalyzer Electropherogram Profile for 8 RNA Samples (Control, LPS, BK and PK).....	43
Figure 14 Correlation Matrix on Aligned Reads.....	45
Figure 15 Principal Component Analysis Plot.....	46
Figure 16 MA plot.....	47
Figure 17 Genome-wide transcriptome heatmap analysis of RNA-Seq derived gene expression data.....	49
Figure 18 Bar graph.....	51
Figure 19 Venn diagram.	60
Figure 20 Pie Chart.....	63

Figure 21 Pie Chart.....	65
Figure 22 Pie Chart.....	67
Figure 23 Effect of Plasma Kallikrein and Bradykinin on Gene Expression.	68
Figure 24 Pathway Studio pathways relating expressed proteins in LPS-stimulated macrophages to distinct proteins, cell processes and diseases.....	70
Figure 25 Pathway Studio pathways relating expressed proteins in PK-stimulated macrophages to distinct proteins, cell processes and diseases.	73
Figure 26 Pathway Studio pathways relating expressed proteins in BK-stimulated macrophages to distinct proteins and diseases.....	76
Figure 27 Relative expression of four receptor genes in bone marrow-derived macrophages.	77
Figure 28 IL-6 and TNF- α secretion by BMDMs after inhibiting PAR receptors.....	79

TABLES

Table 1 Primer sequences and annealing temperatures for select murine genes	35
Table 2 The variation in the regulated gene numbers in the three treated groups	50
Table 3 Comparative list of genes in LPS-stimulated BMDMs for 24 hours compared to control	52
Table 4 Comparative list of genes in BK-stimulated BMDMs for 24 hours compared to control	55
Table 5 Comparative list of genes in PK-stimulated BMDMs for 24 hours compared to control	57
Table 6 List of Altered Pathways in Response to LPS Stimulation	62
Table 7 List of Altered Pathways in Response to BK Stimulation	64
Table 8 List of Altered Pathways in Response to PK stimulation.	66

ABBREVIATIONS

A

APP: Aminopeptidase P

APCs: Antigen-presenting cells

ACE: Angiotensin converting enzyme

ANG II: Angiotensin II

ARG-1: Arginase-1

B

BMDM: Bone marrow-derived macrophages

BKRs: Bradykinin receptors

BK: Bradykinin

C

CPN: Carboxypeptidase N

CVD: Cardiovascular diseases

CCL2: C-C motif chemokine ligand 2

CCL16: C-C motif chemokine ligand 16

CCL17: C-C motif chemokine ligand 17

CCL18: C-C motif chemokine ligand 18

CD: Cluster of differentiation

CSF-1: Colony Stimulating Factor-1

CSF-1R: CSF-1 receptors

D

DAMPs: Damage-associated molecular patterns

DEPC: Diethylpyrocarbonate

DMEM: Dulbecco's Modified Eagle Medium

E

ECM: Extracellular matrix

ELISA: Enzyme-linked immunosorbent assay

F

FXII: Factor 12

F2R: Coagulation Factor II Thrombin Receptor

F2RL1: Coagulation factor II (thrombin) receptor-like 1

F2RL2: Coagulation factor II (thrombin) receptor-like 2

F2RL3: Coagulation factor II (thrombin) receptor-like 3

FBS: Fetal bovine serum

FN1: Fibronectin-1

G

GPCRs: G protein-coupled receptors

H

HSC: Hematopoietic stem cell

HEPES: 4-(2-hydroxyethyl)-1-piperazineethanesulfonic acid

HMWK: High molecular weight kninogen

HRP: Horseradish peroxidase

I

IL-1 β : Interleukin-1 β

IL-4: Interleukin-4

IL-6: Interleukin-6

IL-10: Interleukin-10

IL-12: Interleukin-12

IL-13: Interleukin-13

IL-12: Interleukin-12

IL-21: Interleukin-21

IL-33: Interleukin-12

IL-34: Interleukin-12

IFN- γ : Interferon- γ

IGF-1: Insulin-like growth factor-1

iNOS: Inducible nitric oxide synthase

IMT: Intima-media thickness

K

KLK: Kallikrein

KKS: Kallikrein-kinin system

L

LCM: L929 conditioned medium

LDL: Low-density lipoprotein

LPS: Lipopolysaccharide

M

MHC II: Major histocompatibility complex II

MR: Mannose receptors

MMP: Matrix metalloproteinase

MAPK: Mitogen-activated protein kinase

MI: Myocardial infarction

N

NK: Natural killer

NO: Nitric oxide

P

PAMPs: Pathogen-associated molecular patterns

PBS: Phosphate-buffered saline

PRRs: Pathogen recognition receptors

PK: Plasma kallikrein

PPK: Plasma pre-kallikrein

PCA: Principal component analysis

PANTHER: Protein analysis through evolutionary relationships

PRCP: Prolylcarboxypeptidase

Q

QC: Quality Control

R

ROS: Reactive oxygen species

RBL: Red blood cell lysis

RAS: Renin-angiotensin system

RIN: RNA integrity number

RT-qPCR: Reverse transcription quantitative polymerase chain reaction

RPMI: Roswell Park Memorial Institute

S

SR: Scavenger receptors

T

TMB: 3,3',5,5'-tetramethylbenzidine

TK: Tissue kallikrein

TLRs: Toll-like receptors

TGF- β : Transforming growth factor-beta

TPM: Transcript Per Million

TNF- α : Tumor necrosis factor-alpha

V

VEGF: Vascular endothelial growth factors

VSMCs: Vascular smooth muscle cells

W

WHO: World Health Organization

CHAPTER I

INTRODUCTION

A. Inflammation

1. Overview

Inflammation comes from the root “inflamm”, which is taken from the Latin word *inflammare* (to burn). Although it sounds harmful, inflammation is actually one of the most crucial mechanisms necessitated in the protection and defense of cells against certain injuries or microbial infections (Isailovic, Daigo et al. 2015). Inflammation is an immune response initiated by harmful stimuli such as pathogens, damaged cells, toxic compounds and radiation (Chen, Deng et al. 2018). At the tissue level, it is characterized by swelling, heat, pain and redness (Oishi and Manabe 2016). When an inflammatory response is initiated, several immune cells are triggered and recruited whereby the principal aim is to repair the tissues that have been damaged as well as to remove cellular debris, thereby allowing for the re-establishment of normal homeostasis (Serhan, Brain et al. 2007).

Tissue repair and regeneration are critical biological processes that are fundamental to the survival of all living organisms (Das, Sinha et al. 2015). Hence, inflammation is considered as an essential defense mechanism for maintaining health and, therefore, it is vital for the human body and the regeneration of injured tissues (Sansbury and Spite 2016). When tissues are damaged during an infection or following a mechanical wound, inflammation is stimulated as a response to damage-associated molecular patterns (DAMPs) and pathogen-associated molecular patterns (PAMPs) that are released by dead cells and invading organisms, respectively (Zhang, Raoof et al. 2010). These molecular

triggers, in turn, induce a complex inflammatory response which is described by the recruitment and activation of a variety of hematopoietic and non-hematopoietic cells including neutrophils, macrophages, natural killer (NK) cells, B-cells, T-cells, fibroblasts and endothelial cells that together build up the cellular response which coordinates tissue repair (Wynn 2008). In such circumstances, vasodilation takes place, thereby increasing blood flow carrying immune cells to the injured area, leading to vascular permeability. The aforementioned mechanism is what contributes to acute inflammation and tissue homeostasis. Moreover, when the wound healing process is well organized and controlled, the inflammatory response resolves thereafter, and normal tissue architecture is restored. However, in cases where the inflammation is neither resolved nor controlled, acute inflammation is able to progress to chronic inflammation causing greater tissue damage, tissue remodeling disorders, and poor tissue healing, and may last for several weeks or months (Greaves and Channon 2002). These conditions are known to induce the transition to chronic and maladaptive inflammatory pain (Ji, Xu et al. 2011) and may result in several pathologies, including cancer and fibrosis (Karin and Clevers 2016), in addition to vascular and neurological diseases (Greaves and Channon 2002). Although different inflammatory processes exist, they all share common mechanisms. These mechanisms include the recognition of detrimental stimuli by cell surface receptors, the activation of inflammatory pathways, the release of inflammatory markers and the recruitment of inflammatory cells.

2. *Immune Cells in Inflammation*

In healthy individuals, the innate immune system offers the first line of host defense against either external or internal threat *via* the initiation of a protective inflammatory response which cultivates during time through different phases. Moreover, in order to maintain systemic homeostasis, the human body relies on immune cells that aim at resolving inflammation in a regulated manner (Mosser and Edwards 2008). This phenomenon is accomplished by the instantaneous removal of foreign and endogenous pathogens, as well as the maintenance of wound healing and tissue repair (Varga, Mounier et al. 2016). Inflammatory phases include the initiation of inflammation as well as the resolution and re-establishment of tissue integrity (Italiani and Boraschi 2014). Initially, the primary stage of inflammatory response is determined to destroy pathogens by phagocytes, followed by a phase where necrotic and dying cells, damaged extracellular matrix material and cellular debris are removed by the cumulative action of several immune cells. In such cases, a final phase known as the recovery phase is introduced, whereby cells are recruited to help promote the tissue repair and restoration to a completely healthy and functional state (Italiani and Boraschi 2014). However, as stated before, in cases where the acute inflammation is not resolved, it might progress to chronic inflammation as its underlying causes and effects persist for an extended period of time (Nathan and Ding 2010).

3. *Macrophages*

Lately, macrophages, a subset of cells of the innate immune system, have become a subject of scientific interest under both physiological and pathological conditions.

Macrophages are an essential part of the immune system that are equipped with a set of pathogen recognition receptors (PRRs). These receptors in turn are able to initiate the phagocytosis of pathogens and the secretion of cytokines as well as chemokines (Gombozhapova, Rogovskaya et al. 2017). Moreover, being regarded to as antigen-presenting cells (APCs), macrophages are able to display antigens on their cell surface through their major histocompatibility complex II (MHC II). Furthermore, macrophages promote resorption of cellular debris, neoangiogenesis and produce pro-inflammatory and anti-inflammatory factors. In several ways, they help regulate cardiac remodeling and healing post myocardial infarction by the secretion of factors such as proteases and growth factors (Nich and Goodman 2014).

a. Origin, Role and Tissue Distribution

In the bone marrow, there resides a niche of multipotent stem cells known as the hematopoietic stem cell (HSC). HSCs have the ability to form all of the cells of the blood and immune system (Fig. 1). As the quintessential stem cells, they are capable of self-replicating and differentiating into progeny of multiple lineages (Weiskopf, Schnorr et al. 2016). These lineages include the lymphoid lineage that gives rise to B- and T-lymphocytes and the myeloid lineage from which monocytes arise. Monocytes are white blood cells that circulate in the bloodstream and migrate into different tissues and organs where they differentiate into tissue and bone marrow-derived macrophages (BMDM) (van Furth and Cohn 1968). Homeostatic control of monocyte and/or macrophage development is predominantly influenced by Colony Stimulating Factor-1 (CSF-1) (also known as

Macrophage-CSF)
 which are produced
 by stromal cells such
 as fibroblasts and
 pericytes (Hamilton
 2008). In turn,
 mature mononuclear
 phagocytes express
 CSF-1 receptors

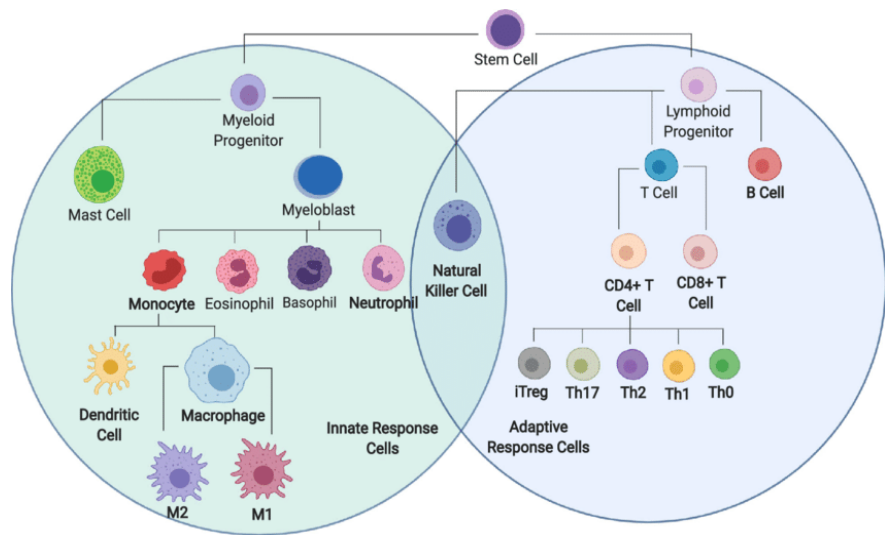


Figure 1 / Immune cell lineage. (adapted from Torang et al. BMC Bioinformatics, 2019)

(CSF-1R) and are thus able to remove circulating CSF-1, allowing a negative feedback loop responsible for the decrease of monocyte proliferation (Tushinski, Oliver et al. 1982). Once monocytes are recruited to the site of injury, they are able to differentiate into macrophages, thereby serving as a source of either classical or alternative macrophages (Jenkins, Ruckerl et al. 2011). As soon as the inflammatory elements are cleared, the majority of macrophages either leave the inflammatory site or undergo apoptosis (Randolph 2009).

b. Phenotypes

To increase the immune defensive firepower, there occurs an increase in the effector cell number in the tissue during the first phases of inflammation. These cells are known as bone marrow-derived macrophages (Italiani and Boraschi 2014); primary macrophage cells that derive from circulating monocytes in the presence of growth factors. Central to the issue of

monocyte recruitment is the difference in monocyte subset trafficking. Depending on the physiological environment, different subsets of macrophages displaying several degrees of activation are generated. The exposure of macrophages to interferon- γ (IFN- γ) and their recognition of PAMPs such as lipopolysaccharide (LPS), chitin, and other intracellular pathogens induces their polarization into M1 macrophages (Fig. 2). In addition to PAMPs, DAMPs that result from either tissue or cell damage and necrosis may also promote inflammation. Both types of molecular patterns bind to pattern recognition receptors located on the surface of macrophages. An example of these receptors which are associated with macrophage activation are toll-like receptors (TLRs) (Mogensen 2009). On the other hand, the exposure of macrophages to cytokines such as interleukin-4 (IL-4) and/or interleukin-13 (IL-13) induces their differentiation into M2 macrophages (Binder, Hayakawa et al. 2013). As such, the stimulation of macrophages leads to the production of distinct functional phenotypes which are analogous to the Th1/Th2 T-cell polarization paradigm (Yap, Cabrera-Fuentes et al. 2019). Therefore, it can be stated that M1 macrophages which are also known as “classically activated” cells are representative of pro-inflammatory characteristics. The activity in M1 macrophages results in the transcription of nitric oxide (NO) and reactive oxygen species (ROS). Since they are known to be

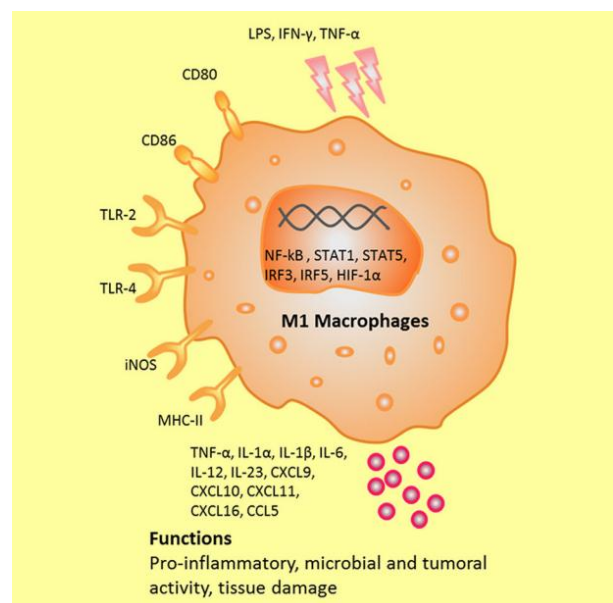


Figure 2 / Activation markers and effectors of M1 macrophages. (adapted from Yao et al. *Frontiers in Immunology*, 2019)

pro-inflammatory cells, they release cytokines such as interleukin-1 β (IL-1 β), interleukin-6 (IL-6), interleukin-12 (IL-12), and tumor necrosis factor-alpha (TNF- α), and chemokines such as C-C motif chemokine ligand 2 (CCL2) which are involved in immune cell recruitment and invasion (Bettelli, Carrier et al. 2006). These macrophages express surface markers known as cluster of differentiation (CD), of which include CD40, CD80 and CD86 (An, An et al. 2019).

M2 macrophages or “alternatively activated” macrophages are representative of anti-inflammatory characteristics and are associated with tissue repair, in addition to wound healing (Mantovani, Sozzani et al. 2002). The term “alternatively activated” denotes an activation different from the “classically activated” one. Hence, it must be acknowledged that M2 macrophages indeed exhibit a growing spectrum of phenotypic and functional varieties, which are detailed further below (Nich and Goodman 2014). Alternatively activated macrophages promote collagen synthesis, fibrosis, and other tissue remodeling functions (Pesce, Ramalingam et al. 2009). M2 macrophages display increased expression of receptors such as mannose receptors (MR) which are also known as CD206 and scavenger receptors (SR) (Yap, Cabrera-Fuentes et al. 2019). They are also involved in proteolytic enzymes release, including matrix metalloproteinase (MMP) such as MMP-2 and MMP-9 that result in the degradation of collagen as well as elastin and fibronectin. Moreover, alternatively activated macrophages have the capability of secreting transforming growth factor-beta (TGF- β) which stimulates the differentiation of myofibroblasts into fibroblasts thereby contributing to the synthesis and deposition of extracellular matrix and collagen. In addition to TGF- β , these types of macrophages secrete anti-inflammatory cytokines like IL-10, chemokines like CCL17 and CCL22 and the

enzyme arginase-1 (ARG-1) which is involved in cell proliferation, collagen formation, and tissue repair (Pesce, Ramalingam et al. 2009; An, An et al. 2019). The polarization of macrophages into M2 cells is usually accomplished by the activation of IL-10 receptor (IL-10R1) and antigens recognized by the Fc family of receptors (Mantovani, Sica et al. 2004). Besides the down-regulation of several pro-inflammatory cytokines which are implicated in M1 stimulation, IL-4 and IL-13 induce fibrogenesis by the expression of fibronectin-1 (FN-1) and beta 2 integrin (ITGB2) (Hart, Burgess et al. 1989). However, lately it has been shown that other mediators such as IL-21, IL-33 and IL-34 may also drive the polarization of alternative macrophages (Randolph 2009; Biglu, Ghavami et al. 2016). Additionally, alternatively activated macrophages modulate tissue repair and cell proliferation signaling via insulin-like growth factor-1 (IGF-1) (Gratchev, Guillot et al. 2001).

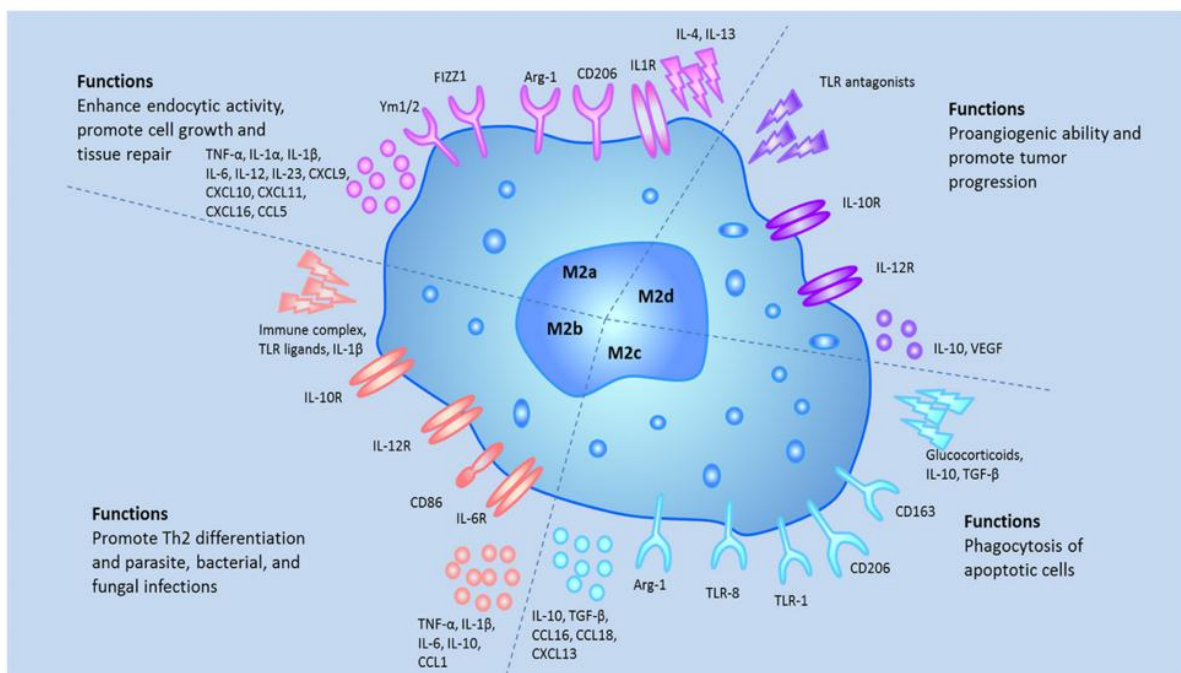


Figure 3 / Activation markers and effectors of M2 macrophages. (adapted from Yao et al. *Frontiers in Immunology*, 2019)

It is fundamental to mention that in 2004, M2 macrophages were further subcategorized into M2a, M2b, M2c and M2d cells as illustrated in Fig. 3 (Nahrendorf and Swirski 2013) depending on the applied stimuli and the induced transcriptional changes where their characterization highlighted general properties and activation processes (Nahrendorf and Swirski 2013). To begin with, M2a macrophages result in an elevated expression of IL-10, TGF- β , CCL17, CCL18, and CCL22. These macrophages lead to tissue repair, cell growth and enhance the endocytic activity (Yao, Xu et al. 2019). On the other hand, M2b macrophages are not only capable of releasing anti-inflammatory factors, but pro-inflammatory cytokines as well. These mediators include TNF- α , IL-1 β , IL-6, and IL-10. Furthermore, M2c cells, also known as inactivated macrophages, stimulate the release of IL-10, TGF- β , CCL16, and CCL18. These cells play an essential role in the phagocytosis of apoptotic cells (Chistiakov, Bobryshev et al. 2015). Finally, M2d macrophages result in the secretion of IL-10 and vascular endothelial growth factors (VEGF) whereby they are able to promote angiogenesis (Ferrante, Pinhal-Enfield et al. 2013).

B. Cardiovascular Diseases

1. Overview

When studying causes of death in the world, cardiovascular diseases (CVD) are a major aspect to consider, because they are the leading cause of mortality globally and a major barrier to sustainable human development (Clark 2013). According to the World Health Organization (WHO), a higher percentage of people die yearly from CVDs than any other disease. Cardiovascular disease is not merely a disease, but rather composed of several disorders that involve the heart and blood vessels. Some of these disorders include

coronary heart disease, congenital heart disease, deep vein thrombosis and pulmonary embolism and angina. CVD is the main reason behind a large number of deaths among males and females below the age of 75 (Cowie 2017). Moreover, in 2016, it was estimated that around 17.9 million people died from CVDs, representing 31% of all global deaths, whereby 85% of these deaths were due to stroke and myocardial infarction ((WHO) n.d). Furthermore, it has been predicted that approximately 23.6 million people will die annually from CVD by the year 2030 (Lauer, Kiley et al. 2015). Not only is the rate of mortality high, but the financial burden of patients to be treated for CVD is extremely high (Biglu, Ghavami et al. 2016).

2. *Myocardial Infarction*

A heart attack or what is also known as myocardial infarction (MI) occurs when one of the heart's coronary arteries has extremely slow blood flow or is suddenly occluded (Fig. 4). When a coronary artery is completely or partially occluded, it creates a severe reduction in the

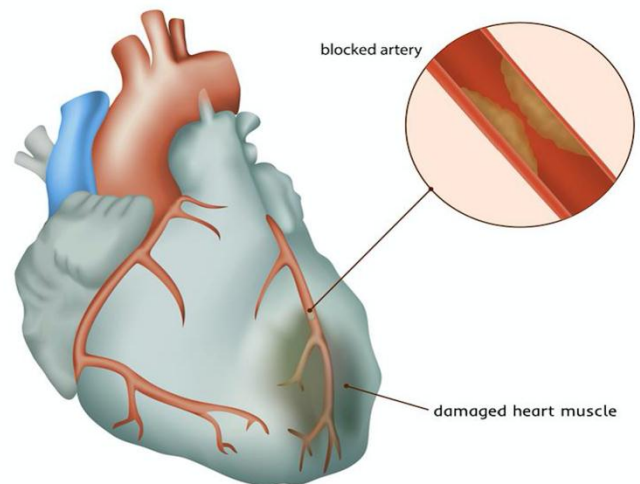


Figure 4 | Anatomy of a heart attack. (adapted from Warriner and Al-Matok, 2019)

blood flow, resulting in some of the heart muscle being irrigated by that artery to become infarcted (Goldstein, Demetriou et al. 2000). The sudden blockage of a coronary artery usually occurs due to the formation of a blood clot or what is also known as

a thrombus, which may result from plaques that build up along the inner walls of blood vessels.

The following phenomena will lead to a depletion in oxygen delivery throughout the coronary artery, which in turn would bring about a decreased oxygenation of the myocardium itself (Haig, Carrick et al. 2019). Additionally, rupture of atherosclerotic lesions culminates the formation of thrombus, as well as platelet aggregation. Myocardial infarction occurs as an irreversible damage to the myocardium or cardiac muscle, due to oxygen depletion. It is when ischemia is of sufficient duration to induce myocyte necrosis (Alan J. Mouton 2018). On the other hand, an MI may also occur without the formation of a blood clot, which is when the demand for oxygen in a patient is greater than that which is being supplied.

a. Epidemiology

The most severe manifestation of coronary artery disease is known to be MI as it is one of the leading reasons behind death in the world. MI occupies a substantial footprint on global health, thereby impacting each year over 7 million individuals worldwide (Weintraub, Daniels et al. 2011). Although the prevalence of the disease approaches more than 2.4 million deaths in the USA, it results in more than 4 million deaths in Europe and northern Asia (Nichols, Townsend et al. 2014). Moreover, it contributes to more than third of deaths yearly in developed nations (Yeh, Sidney et al. 2010). However, in recent decades, the increased use of therapies and changes in lifestyles, mitigated the mortality from coronary heart disease (Nichols, Townsend et al. 2014). In 2014, based on the self-

reported national survey of the UK, the prevalence of MI was reported as 640,000 in men and 275,000 in women, thereby representing about 915,000 people that have suffered an MI in the UK. Furthermore, in 2013, the prevalence of MI in men was about three times higher than that in women in the UK (Bhatnagar, Wickramasinghe et al. 2015). In contradiction to the developed countries, South Asian countries such as India, Pakistan, Sri Lanka, Bangladesh, and Nepal have the greatest prevalence of MI seen in people younger than 45 years of age as opposed to people older than 60 years of age. Out of all patients suffering from MI, 70% of serious incidents occur as a result of occlusion from atherosclerotic plaques. Several risk factors that predispose the development of CVDs, are divided into 2 types. The first type of risk factor is the modifiable ones which includes cigarette smoking, exercise, hypertension, obesity, low-density lipoprotein (LDL), and triglyceride levels. Moreover, this type of factor accounts for 90% in males and 94% in females. However, non-modifiable risk factors include age, sex, genetic factors and family history (Berg, Wiviott et al. 2018).

b. Pathology

As soon as myocyte ischemia takes place, and necrosis has commenced, an inflammatory response is triggered through the death of myocytes. In order to get rid of necrotic debris, the myocardium goes through a wound-healing pattern or model. Initially, this process involves aspects such as pro-inflammatory and extracellular matrix (ECM)-degrading components. Since the heart of humans has negligible regenerative capacity, cardiac damage possesses a massive challenge for the reparative means of the body,

eventually resulting in scar formation (Frangogiannis 2008). So as to minimize the inflammation and stimulate ECM deposition, anti-inflammatory and pro-reparative factors come into play, thus forming new scars. These factors or players include cardiac myocytes, neutrophils, macrophages, fibroblasts, and endothelial cells, with cross-talk taking place through all cell types. However, the fibroblasts along the macrophages have essential roles in post-MI wound healing whereby they provide mediators that span the whole period of the response (Alan J. Mouton 2018). Healing after infarction can be divided into three phases, the first being the inflammatory phase, whereby there occurs an activation of chemokine as well as cytokine cascades. These cascades then lead to the recruitment of leukocytes, neutrophils and macrophages into the infarcted area (Frangogiannis 2008). After this stage comes the proliferative phase where the pro-inflammatory mediators are suppressed. In this case, there is a proliferation of fibroblasts and endothelial cells (Frangogiannis 2006). At this stage, extracellular matrix proteins are produced by differentiated myofibroblasts. Finally, the maturation phase takes place whereby vascular cells and fibroblasts undergo apoptosis, followed by the deposition of collagen-based scars (Frangogiannis 2008). When cells die due to necrosis, they express intracellular mediators (DAMPs) thereby eliciting a profound inflammatory response through the activation of innate immune mechanisms as well as a cascade of inflammatory pathways. Multiple receptors sense the endogenous ligands being released at the time of injury, thus activating inflammatory pathways. Farther than being just some kind of “warning system”, the innate immunity is a complex molecular network that is sensitive to several signaling molecules which are released during cell necrosis and degradation of extracellular matrix components (Gombozhapova, Rogovskaya et al. 2017). A universal response to an increased wall stress

and loss of the viable myocardium is cardiac remodeling. Cardiac remodeling takes place following myocardial infarction as a course of modifications in cardiac activity and structure (Opie, Commerford et al. 2006).

c. Integration of Macrophages

The heart is a complex tissue consisting of multiple cells with different cell types. One third of the cells residing in the myocardium are cardiomyocytes (Perbellini, Watson et al. 2018). The remaining two thirds are cells such as fibroblasts, smooth muscle cells, endothelial cells and macrophages that are responsible for matrix deposition and vascularization (Fountoulaki, Dages et al. 2015; Wang, Kit-Anan et al. 2018). All these types of cells communicate biochemically through signals such as cytokines and growth factors (Fountoulaki, Dages et al. 2015). Moreover, the massive quantity of cell death after MI is detrimental, since the heart has a limited regenerative capacity (Isomi, Sadahiro et al. 2019). In order to compensate for the loss of cells and maintain the integrity of the heart, the cardiac tissue experiences considerable remodeling. Hence, inflammatory stimulation promotes the removal of necrotic cells as well as tissue remodeling (Frangogiannis 2015). A major hallmark of myocardial infarction is the infiltration of bone marrow-derived macrophages to the infarct zone. This can be illustrated through stages of macrophage infiltration and their distinctive roles within the myocardium (O'Rourke, Dunne et al. 2019). In this sense, following MI, resident cardiac macrophages start to undergo necrosis due to ischemia, with a total loss of the cardiac macrophages 24 hours post MI (Heidt, Courties et al. 2014). However, that being said, resident cardiac macrophages which are

lost in the ischemic region are replaced within 24 hours by infiltrating of BMDM (Heidt, Courties et al. 2014). Although the precise mechanism behind post-MI in vivo macrophage polarization is not well understood, Nahrendorf et al. previously recognized sequential infiltration of monocyte subsets into the ischemic heart (Nahrendorf, Swirski et al. 2007). Furthermore, they also found that early recruitment of monocytes relies on CCR2 secreted by resident cells in the heart, whereas later recruitment depends on CX3CR1 (Dutta and Nahrendorf 2015). Moreover, the microenvironment in the infarcted area is occupied with early pro-inflammatory mediators like IFN- γ , whereas later anti-inflammatory mediators such as IL-4 and IL-10 are secreted which in turn directs the polarization of macrophages into either M1 or M2 (Christia, Bujak et al. 2013; Jung, Ma et al. 2017). As early as 30 min following MI, circulating monocytes reach the infarcted region (Jung, Kim et al. 2013). Bone marrow-derived macrophages may possess different polarization phenotypes. M1 cells or pro-inflammatory macrophages dominate the heart the first 3 days post-MI whereby they drive acute inflammation and facilitate the clearance of necrotic cells. M1 macrophages release pro-inflammatory cytokines, chemokines, and growth factors so as to aid in clearing cellular debris (ter Horst, Hakimzadeh et al. 2015). Nevertheless, sustained activation of M1 macrophages may result in the delayed resolution of inflammation as well as the delayed formation of scar, in addition to the expansion of the infarct size (Leuschner, Dutta et al. 2011). On the other hand, M2 macrophages, working to resolve the inflammation and promote ECM remodeling are the main cells at days 5–7 post-MI. (Yan, Anzai et al. 2013). Therefore, these types of macrophages are regarded as pro-reparative (ter Horst, Hakimzadeh et al. 2015). M2 macrophages have the capability to produce anti-

inflammatory cytokines like IL-10, proangiogenic mediators like EGF and pro-reparative/fibrotic factors such as TGF- β .

d. Prognosis

Unfortunately, myocardial infarction still holds a high mortality rate, whereby most of the death cases take place prior to arrival to the hospital. Moreover, at least 5% to 10% of MI survivors pass away within the primary 12 months post-MI, whereas around 50% necessitate hospitalization throughout the same year (Mechanic OJ 2019).

e. Therapies

Despite the fact that there are no definitive cures for myocardial infarction, there have been many advances regarding its therapies and treatments. Hence, one way of acute management is reperfusion therapy whereby fibrinolysis takes place (Roffi, Patrono et al. 2016). Nevertheless, if and when fibrinolysis is to take place, it must be carried out with specific agents like tenecteplase or alteplase (Ibanez, James et al. 2018). In addition to the enzymatic breakdown of the fibrin in the blood clot, nitrates are also used either intravenously or sublingually in order to relieve patients from symptoms such as high blood pressure (Ibanez, James et al. 2018). Moreover, Aspirin is usually suggested as an oral medication since this drug is known to inhibit platelets from producing the pro-thrombotic Thromboxane A₂ or TXA₂ (Patrono, Morais et al. 2017). Besides Aspirin, beta-blockers which reduce the impact of circulating catecholamines such as epinephrine can be used. Beta-blockers are able to diminish the consumption of myocardial oxygen through their action on decreasing myocardial contractility, heart rate and blood pressure, whereby they

inhibit beta receptors in patients suffering from cardiovascular diseases (Jan. 2019). It is noteworthy to mention that there are long-term management therapies like angiotensin converting enzyme (ACE) inhibitors that are prescribed to people with heart failure or hypertension which aid in lowering levels of angiotensin II (ANG II) as well as dilating blood vessels thereby increasing blood-flow, in addition to lipid-lowering treatments or statins that are usually administered in order to reduce LDLs (Ibanez, James et al. 2018). Finally, patients with heart problems might consider modifying their lifestyles. To illustrate, cessation of smoking is known to be the most cost-effective secondary measure to prevent MI. Moreover, in a study performed by Ojha et al., they found that smoking does indeed have a pro-thrombotic effect, which in turn has a strong association with atherosclerosis and myocardial infarction (Anand, Islam et al. 2008). Likewise, controlling one's diet and weight as well as performing physical activities are major aspects to consider, since they can really lower the risk of having an infarction (Piepoli, Hoes et al. 2016).

C. Kallikrein-Kinin System

The plasma kallikrein-kinin system (KKS) plays a fundamental role in many mechanisms including the cardiovascular system. Moreover, the KKS has several components which possess distinct functions depending on the type and intensity of the stimulus. As such, the activation of this system has the capability to induce genes and activate biomolecules which are implicated in the molecular mechanisms lying behind vasodilation, blood coagulation and fibrinolysis (Bryant and Shariat-Madar 2009).

1. Plasma Kallikrein: Synthesis, Structure and Function

Although plasma kallikrein (PK) is a serine protease synthesized predominantly in the liver as a glycoprotein zymogen known as plasma pre-kallikrein (PPK) (Kolte 2016). PK is also referred to as Fletcher factor, after the Fletcher family who appeared to have a hereditary deficiency in an unknown coagulation factor, and is encoded by a gene localized to the q34–q35 region on the long arm of chromosome 4 (Beaubien, Rosinski-Chupin et al. 1991). Plasma kallikreins are kininogenases which produce kinins through the hydrolysis of substrates known as kininogens that circulate in plasma. Around 75%-90% of PK circulates in the plasma bound to high molecular weight kininogen (HMWK) (Hock, Vogel et al. 1990; Herwald, Renne et al. 1996). PPK is able to transform into its active form, plasma kallikrein via several ways. PPK is activated mainly by a fragment of factor XII known as α FXIIa. Both the plasma protease precursors factor XII (FXII) and plasma pre-kallikrein (PPK) experience reciprocal proteolytic conversion to the fully active protease species alpha factor XIIa (α FXIIa) and α -kallikrein (α -kal) on anionic surfaces (Bates and Weitz 2005; Wheeler and Gailani 2016). However, it can also be activated by prolylcarboxypeptidase (PRCP) on endothelial cells (Cochrane and Griffin 1979; Shariat-Madar, Mahdi et al. 2002) and by vascular smooth muscle cells (Keum, Jaffa et al. 2014). The activation of plasma kallikrein occurs as the bond between Arg371 and Ile372 is cleaved, leading to the exposure of protease binding domain containing two subunits having a light and a heavy chain linked via a disulfide bond and therefore revealing its catalytic activity (Feener, Zhou et al. 2013). Furthermore, PK is implicated either through its downstream effectors or by itself in several signaling pathways. As such, PK might intersect in the KKS, the fibrinolytic pathway, the alternative complement system and the

renin-angiotensin system (RAS) (Bjorkqvist, Jamsa et al. 2013).

2. *Receptors*

a. Bradykinin Receptors (BKR)

Vasodilation, smooth muscle contraction and pain induction are physiological effects that are known to be exerted by biological active peptides known as kinins. Kinins are generated from a precursor

protein called kininogen

(Fig. 5), which can be

cleaved by kallikreins

(KLKs). There are a wide

range of kinin peptides in

mammalian species, however, the two most investigated members of the kinin family are

bradykinin (BK) and kallidin. Once formed, kinins are degraded by kininases such as

kininase II, which is the same as angiotensin-converting enzyme or ACE (Tschope, Gohlke

et al. 1997). Kinins employ their effect through their cell surface G protein-coupled

receptors (GPCRs) known as BK B1 receptor (B1R) and/or B2 receptor (B2R) after

stimulation. Unlike B1R that has a greater affinity for the carboxypeptidase metabolites of

kinin, des-Arg⁹-BK, B2R is receptive to the kinin BK (Tschope, Gohlke et al. 1997).

Bradykinin is a nonapeptide that is rapidly metabolized by the action of numerous endogenous metalloproteases like ACE, carboxypeptidase N (CPN) and aminopeptidase P



Figure 5 / Cleavage of kininogen into bradykinin. (adapted from Sexton et al. JACI, 2019)

(APP) (Maurer, Bader et al. 2011). Furthermore, the B2R is constitutively expressed while B1R is an inducible receptor (Maurer, Bader et al. 2011; Pereira, Felizardo et al. 2014). Upon binding of bradykinin to the aforementioned receptors, a plethora of downstream effects take place including increased vascular permeability, vasodilation, reduction of oxidative stress through the release of NO on endothelial cells and increased intracellular calcium (Ca^{2+}) concentration (Maurer, Bader et al. 2011).

b. Protease-Activated Receptors (PARs)

The majority of the cellular mechanisms performed by kallikrein are believed to be mediated through either BK 1 receptor and/or BK 2 receptor through which BK acts upon.

Nonetheless, in a study conducted by Abdallah et al., it was reported that the exposure of vascular smooth muscle cells (VSMCs) to PPK was able to activate the cells through the ERK1/2 mitogen-activated protein kinase (MAPK)

pathway. This was seen by a

process that necessitates plasma kallikrein, however without implicating bradykinin receptors (Abdallah, Keum et al. 2010). As such, they demonstrated that PK has the capability to directly activate protease activated receptors 1 and 2 (PAR1/2), that contain consensus kallikrein cleavage sites (Abdallah, Keum et al. 2010). PARs are a type of

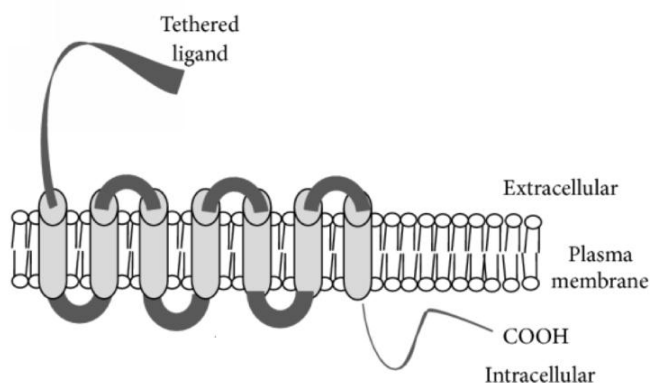


Figure 6 / Protease activated receptors. (adapted from Kagota et al. Biomed Res Int, 2016)

GPCRs that are exclusively activated by proteolysis (Soh, Dores et al. 2010). Furthermore, these receptors are mainly found in vascular, immune and epithelial cells, as well as astrocytes and neurons, whereby they stimulate distinct cellular responses (Russo, Soh et al. 2009). Several recent studies have found that PARs are fundamental modulators of homeostasis and thrombosis in addition to inflammation (Urban J 2007). PARs are unique receptors as they lack physiologically soluble ligands. They are activated by N-terminal proteolytic cleavage. Once cleaved, the resulting N-termini will act as a ligand which is “tethered” as it interacts with the extracellular loop domain, initiating a signal transduction (Fig. 6) (Heuberger and Schuepbach 2019). Furthermore, the stimulation of PAR receptors may result in the transactivation of other receptors such as co-localized PARs, ion channels, and toll-like receptors (Heuberger and Schuepbach 2019). The four members of the PAR family PAR1-PAR4 are encoded by the genes F2R (Bahou, Nierman et al. 1993) F2RL1 (Nystedt, Emilsson et al. 1994) F2RL2 (Schmidt, Nierman et al. 1998) and F2RL3 (Kahn, Zheng et al. 1998) respectively.

3. KKS in Pathology

Multiple elements of the KKS have been associated in several diseases over the years. These diseases include diabetes, central nervous system diseases and cardiovascular diseases, including thrombosis and atherosclerosis. A study conducted by Patrassi et al., found that the kallikrein-kinin system is activated in diabetic individuals, as there was an increase in the activity of PPK and factor XII in these patients (G, R et al. 1982). Another study on diabetes demonstrated that blocking the mediators of the KKS was an efficient

method to attenuate retinal vascular permeability (Abdulaal, Haddad et al. 2016). A final study on diabetes and CVD performed by Jaffa and Luttrell, showed that circulating levels of plasma pre-kallirein are associated with carotid intima-media thickness (IMT) and its progression in subjects with type 1 diabetes. Their findings indicate that PPK is an independent risk factor for cardiovascular complications in subjects with type 1 diabetes (Jaffa, Luttrell et al. 2016). Furthermore, a study performed on mice by Clermont et al., showed that knocking out PPK gene (KLKB1) is not only well tolerated, but also protective in cases of diabetes-induced retinal vascular hyper-permeability (Clermont, Zhou et al. 2013). In addition to diabetes, kallikreins also play a major role in atherosclerosis. To illustrate, tissue kallikrein (TK) levels were previously found to be important biomarkers for the diagnosis and monitoring of atherosclerosis (Porcu, Emanuelli et al. 2004). Moreover, in 2007, Govers-Riemslog et al. discovered that higher levels of inhibitory complexes of the KKS enzymes reduced the risk of congenital heart diseases as well as stroke in middle-aged men. This was seen as low quantities of both kallikrein C1-inhibitor and FXIIa C1-inhibitor complexes were correlated with augmented risk of cardiovascular problems in patients (Govers-Riemslog, Smid et al. 2007).

Aims of the study

As discussed previously, our current understanding on the plasma kallikrein-mediated inflammatory processes is very lagging. Furthermore, the KKS has been implicated in the pathogenesis of several cardiovascular diseases. However, its exact role and mechanism of action are yet to be defined. We postulate that PK may be involved in the inflammatory processes which occur in CVDs such as myocardial infarction, by acting on the main players of inflammation, BMDM. Our aim in this thesis project is to characterize and assess the inflammatory markers involved in the pathogenesis of CVD upon stimulation with plasma kallikrein. To achieve this goal, we examined the following aims:

- To isolate, culture and stimulate bone marrow-derived macrophages in vitro with bradykinin and plasma kallikrein.
- To detect and measure protein levels of inflammatory factors secreted by stimulated bone marrow-derived macrophages.
- To delineate differentially expressed gene features in response to plasma kallikrein- and bradykinin-treated macrophages compared to untreated ones.
- To uncover the processes underlying the plasma kallikrein-mediated inflammatory pathway by performing pathway analysis.

- To verify bradykinin and protease-activated receptors expression in bone marrow-derived macrophages.
- To identify the receptors in plasma kallikrein-induced inflammation.

CHAPTER II

MATERIALS AND METHODS

A. Bone Marrow-Derived Macrophages

1. Isolation and Culture

Male C57BL/6J mice, 8-10 weeks old (Animal Facility at AUB) were sacrificed in the CO₂ chamber. Briefly, bone marrow cells were harvested from the femurs and tibias of mice (Fig. 7). After the bones were cautiously cleaned, they were flushed with 10mL Roswell Park Memorial Institute (RPMI) (Sigma-Aldrich) complete media (10% FBS, 1% P/S, 1% L-glutamine, 1% HEPES), using 25G needles. The content was then spun down for 5 minutes at 1,500rpm so as to flush down the cells. After centrifugation, the pellet was re-suspended in 2ml Red Blood Cell Lysis (RBL) (Sigma-Aldrich) buffer (diluted to 1X in PBS without Calcium or Magnesium) and incubated for 5 minutes at room temperature. In order to neutralize the RBL buffer, 5ml of RPMI complete media was added and again the cells were briefly centrifuged for 5 minutes at 1,500 rpm. Furthermore, 4ml of RPMI complete media was pipetted into the pelleted cells, which were then distributed equally upon eight petri-dishes whereby each petri-dish had 20% L929 Conditioned Medium (LCM) (obtained from cells overexpressing Macrophages Colony Stimulating Factor) and 5ml RPMI complete media. Finally, the plates were placed in an incubator with CO₂ levels set to 5% and temperature to 37°C. M-CSF was obtained from L929, cells cultured in

Dulbecco's Modified Eagle Medium Phosphate Buffered Saline (DMEM, Sigma-Aldrich) containing 10 % FBS at 37 °C for 10 days.

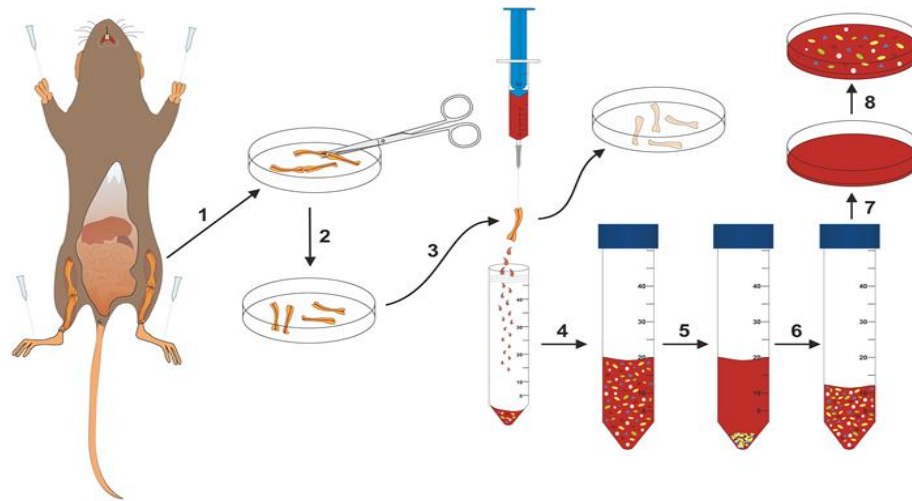


Figure 7 / Representation of the process of isolating and culturing of BMDM from mice. (adapted from Meurer et al. PLOS ONE, 2016)

2. Splitting and Plating

Five days post isolation, media from each petri-dish were aspirated in furtherance to remove of the floating granulocytes. Additionally, for the seeding of the cells, 2ml complete RPMI media was pipetted into each petri-dish, followed by scraping in order to detach all the adhering macrophages. The content of each plate was then collected into a conical tube, whereby it was then subjected to counting. The cells were finally plated in such way that each well in the 12-well plate had 1.5 million cells.

3. Treatment

To allow the cells to adhere onto the plates, treatment was applied 24 hours after seeding. When treating, we first changed the media of each plate and added RPMI only (not complete) to each well. Afterwards, each well was treated with its designated drug (Fig. 8).

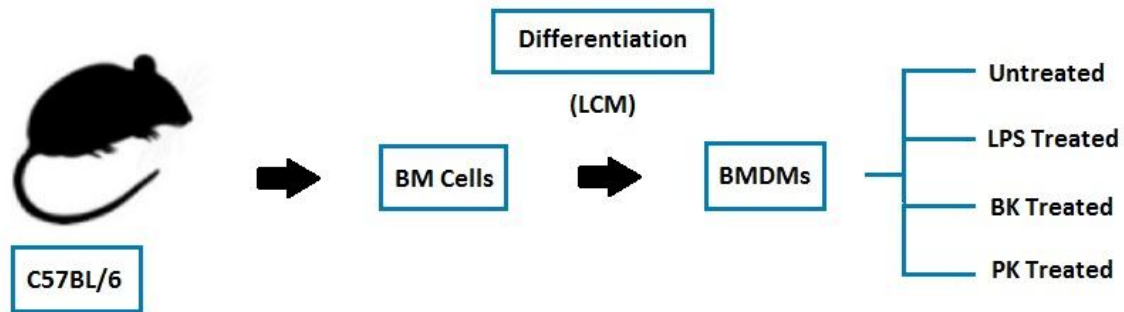


Figure 8 | Experimental design of BMDM treated cells.

B. Stimulation

1. Treatment Concentration

Primary bone marrow macrophages were treated with LPS (10 ng/mL) as a positive control, BK (10^{-7} M) and PK (2.5ng/mL) for 24 hours.

2. Receptor Antagonists Concentration

PAR-1 antagonist (SCH530348) and PAR-2 antagonist (GB83) were purchased from Axon Medchem BV, Cedarlane and used at 0.5 and 2 μ M, respectively. The inhibitors were diluted in RPMI-cultured BMDM from their initial stock of 2030 and 1822 μ M. 30

minutes prior to stimulating with PK, cells were treated with the receptor antagonists, after-which PK was added for 24 hours.

C. Total RNA Extraction

Total RNA was extracted using TRIzol™ Reagent (Ambion; Life Technologies), according to the manufacturer's protocol, after the 24-hour treatments had passed. Moreover, all steps were performed on ice, unless stated otherwise. We first collected the 1mL growth media from each well in the 12-well plate and transferred them into Eppendorf tubes. These tubes were then stored at -20°C, for future use *ELISA*. The cells were washed with PBS (without Ca²⁺/Mg²⁺), which was then aspirated. Each well was scraped thoroughly upon the addition of 500µl of TRIzol™ Reagent. The cell lysates were transferred into Eppendorf tubes whereby they were vortexed for about 30 seconds. 100µl of chloroform were pipetted into each tube, and to ensure homogeneity, they were then vortexed. The tubes were incubated for 5 minutes at room temperature, then centrifuged for 15 minutes at 12,000 × g at 4°C. The aqueous phases (RNA) were pipetted and transferred into new Eppendorf tubes, where 200µl of isopropanol was added for precipitation. The tubes were vortexed for 15 seconds, then left at room temperature for 10 minutes. All samples were then centrifuged for 15 minutes at 12,000 × g at 4°C, after which white gel-like pellets formed (RNA). The supernatants were discarded and 400µl of 75% ethanol was added to each tube, followed by centrifugation for 5 minutes at 7,500 × g at 4°C. The supernatants were then discarded and the prior step was repeated. To guarantee the elimination of all the ethanol, all sample tubes were left to air-dry under the hood at room temperature for 15 minutes. Finally, 20µl of DEPC- treated DNase/RNase-free water

was added to the RNA samples, and then they were placed at 60°C for 5 minutes. To evaluate the purity and concentration of the precipitated RNA, the samples were placed on ice and the absorbance of 1µl of each sample and DNase/RNase-free water (used as blank) were measured using the DeNovix DS-11FX Spectrophotometer. The 260/280 and 260/230 ratios were used to assess the purity of RNA and a ratio of ~2.0 was considered as pure RNA. Lastly, RNA samples were stored at -80°C, until they were used for sequencing.

D. Whole Transcriptome Sequencing Analysis

Using the NextSeq 550 Illumina we performed RNA-Seq of untreated BMDMs and BMDMs which were previously treated with LPS, BK and PK. Each of the four conditions had a biological duplicate (n=2). Briefly, after fragmentation of total RNAs for short read sequencing, RNA samples were reverse-transcribed into cDNA. Adaptors were then ligated onto both ends of the cDNA fragments followed by amplification of the fragments. A representative workflow for RNA-Seq is depicted in Fig. 9. Sequenced raw reads were first subjected to quality control (QC) using FastQC. Since there were reads with a per base sequence quality score less than 20, Trimmomatic was used to remove low quality bases from the 3¹ end, leaving 66 base pairs. Reads were then mapped to the reference mouse genome (UCSC mm10) using Bowtie2 mapping. Transcripts were then assembled from aligned reads using FeatureCounts borrowing from the annotation database `gencode.vM22.annotation_mm10.gtf.gz`. Using DESeq2, we assessed variation patterns within replicates and between conditions *via* Principal Component Analysis (PCA) on counts. To view the association between variables, correlation matrix plots were conducted. Also, significantly differentially expressed features between treated and untreated samples

from count tables were identified. A p-value/p-adjusted value of less than 0.05 was used in order to account for statistical significance. Finally, fold-change threshold of 1 was further applied. With the use of the Transcript Per Million (TPM) method, expression levels within and across samples were compared once raw counts were normalized by scaling gene counts within a sample to a total of 1 million transcripts while also accounting for gene length.

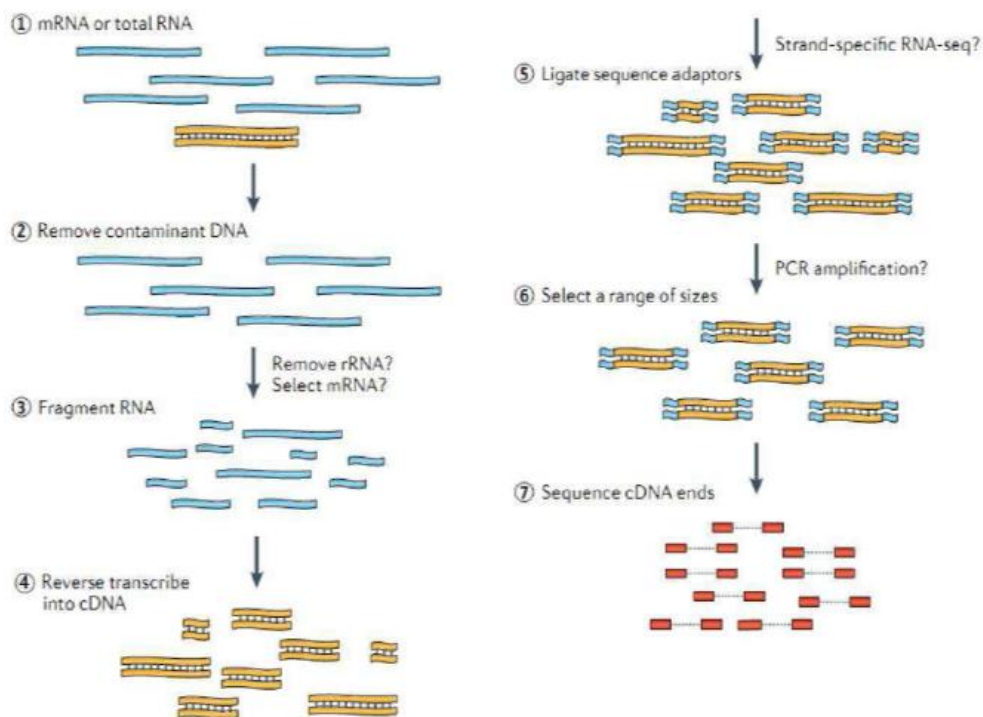


Figure 9 / RNA-Seq experimental workflow (adapted from Martin and Wang Nature Reviews, 2011)

E. Pathway Analysis

Differentially expressed gene features were then functionally analyzed and topologically organized into gene-gene interaction networks using the commercially available software Pathway Studio. This program allows us to examine functional associations among the genes and generate functional (with predicted activated or inhibited states) gene-gene interaction networks based on the presence of inter-connected genes, based on the amount of publications in the software's knowledgebase supporting the connections. The pathways, gene network and gene set analyses permit selection of genes predicted to have key roles in phenotypes (M1 or M2) and diseases based on their expression and number of functional associations within significant interaction networks.

F. Two-step Reverse Transcription Quantitative Polymerase Chain Reaction (RT-qPCR)

In order to validate the differential expression of genes (up-regulated versus down-regulated in plasma kallikrein stimulated cells), we conducted RT-qPCR. The following was done on a total of 11 murine genes (Table 1), according on the magnitude of differential expression.

1. Reverse Transcription of RNA to cDNA

Using the High-Capacity cDNA Reverse Transcription Kit (ThermoFisher Scientific) and according to the manufacturer's protocol, total RNA samples were reverse transcribed to cDNA. RNA samples, as well as the kit reagents were thawed manually, then gently

mixed by flicking the tubes. Before being kept on ice, all tubes were briefly centrifuged in order to collect any residual liquid from the sides of tubes. DNase/RNase-free water was added to 1µg of each RNA sample to a total volume of 14.2µl. Then, the reverse-transcription reaction was performed by preparing a master mix containing all the following components per one reaction:

RT Buffer	2µL
RT Random Primers	2µL
MultiScribe™ Reverse Transcriptase	1µL
dNTP Mix	0.8µL

5.8µL of the master mix was transferred into each tube of template RNA, reaching a total volume of 20µl, then mixed gently. The tubes were then briefly centrifuged and placed in the BioRad T100 Thermal Cycler with Gradient using the conditions below:

Settings	Temperature	Time
Step 1	25°C	10 mins
Step 2	37°C	120 mins
Step 3	85°C	5 mins
Step 4	4°C	∞

Finally, to dilute the cDNA, RNase-free water was added to each tube to get a final volume of 50µl.

2. Quantitative Polymerase Chain Reaction (qPCR)

All the following RT-qPCR experiments were conducted in biological triplicates under sterile conditions, using filtered tips and molecular grade nuclease-free water. The primer oligonucleotide sequences (Table. 1) were manufactured and purchased from Macrogen. All the primer tubes were centrifuged at 1,000 rpm for 1 minute in order to obtain all the lyophilized products in the bottom of the tubes. To reconstitute them and get a stock concentration of 100 μ M, 300 μ L of molecular grade water was added to each tube, then vortexed and centrifuged at 1,000 rpm for a minute. Finally, to obtain a working concentration of 50 μ M, 10 μ L from each stock was taken and dissolved in 10 μ L RNase-free water. The iTaq™ Universal SYBR® Green supermix, DNA samples and primers were left to thaw on ice, mixed thoroughly and centrifuged briefly to collect solutions at the bottom of the tubes. For each transcript reaction, a master mix was prepared on ice according to the following volumes:

Component	Volume (Per 10μL Reaction)
iTaq™ Universal SYBR® Green Supermix	5 μ L
DNase/RNase Free Water	2.3 μ L
Forward and Reverse Primers	0.1 μ L

In order to ensure homogeneity and be able to dispense equal aliquots into all the wells of the PCR plate, the assay master mixes were mixed carefully and spun down. After loading 7.5 μ L of the master mix into each reaction well of a 384-well PCR plate (BioRad),

2.5µl of cDNA was distributed. Since a no-template control was included in each plate reaction, 2.5µl of DNase/RNase free water was added instead of cDNA. Lastly, the PCR plate was sealed using an adhesive sealer, centrifuged at 1,000 rpm for 1 min and loaded into the Real-Time PCR BioRad CFX384 machine. The RT-qPCR thermal cycling conditions which included a melt curve to verify the specificity of the product are summarized below:

Step	Temperature	Time
Polymerase Activation	95°C	5 mins
Denaturation	95°C	10 secs
Annealing	60°C	30 secs
Extension	72°C	30 secs
Melt Curve		5 secs

The obtained data were analyzed using the $2^{-\Delta\Delta C_t}$ calculation method by normalization to Glyceraldehyde-3-Phosphate Dehydrogenase (GAPDH) as a reference gene.

Table 1 | Primer sequences and annealing temperatures for select murine genes

Murine Gene	Annealing Temp. (°C)	Primer Sequence (5'-3')
<i>Bdkrb1</i>	59.90-59.97	F: CCATCAGTCAGGACCGCTAC R: AGGGACGACTTTGACGGAAC
<i>Bdkrb2</i>	59.53-59.17	F: CTGGGTGTTTGGAGAGGTGT R: ACGAGCATCAGGAAGCAGAT
<i>F2R</i>	55.26-57.81	F: TGCATCGATCCGTTGATTTA R: TGCAACTGTTGGGATCAGAG
<i>F2RL1</i>	59.60-59.54	F: TGCTTTGCTCCTAGCAACCT R: CAGAGGGCGACAAGGTAGAG
<i>GAPDH</i>	62.90-69.50	F: CGTCCCGTAGACAAAATGGTGAA R: GCCGTGAGTGGAGTCATACTGGAACA
<i>IL-1β</i>	57.86-58.43	F: GCTGCTTCCAAACCTTTGAC R: TGTCCTCATCCTGGAAGGTC
<i>IL6</i>	58.86-57.24	F: AGTTGCCTTCTTGGGACTGA R: TCCACGATTGCCAGAGAAC
<i>Lgal-3</i>	58.03-58.20	F: ACAAGTCCTGGTGAAGCTG R: GCTGGTGAGGGTTATGTCAC
<i>TNF-α</i>	60.00-61.00	F: CTAGTTTCCTGGTCTGGAGAAGATC R: CCCTCTCCACCAGTCTCCTCTA
<i>MMP-9</i>	58.40-60.50	F: AAAGGCCATTCGAACACCAC R: ATGATGGTCCCACCTTGAGGC
<i>iNOS</i>	60.50-62.50	F: CCTGGAGGTGCTTGAAGAGT R: GGGGCTTCAAGATAGGGAGC
<i>CCL2</i>	57.80-52.60	F: GGGCCTGCTGTTACAGTT R: CCAGCCTACTCATTGGGAT

G. Enzyme Linked Immunosorbent Assay (*ELISA*)

To detect and quantify protein levels secreted by BMDM cells, Invitrogen IL-6 and TNF- α Uncoated *ELISA* Kits were used according to the manufacturer's instructions. Briefly, the capture antibody (250X) was diluted in the coating buffer. The *ELISA* plate was then coated with 100 μ L of the diluted anti-mouse capture antibody, sealed and placed at 4°C overnight. Around 24 hours later, the plate was washed 4 times using a wash buffer prepared by diluting PBS (1X) in distilled water containing Tween20. In order to reduce any background interference and block any non-specific binding sites, the *ELISA* diluent (5X) was diluted to 1X in distilled water, after which 200 μ L were pipetted to each well. The plate was then incubated for an hour at room temperature. Meanwhile, samples were diluted according to previous optimizations. Serial dilution of the standards was conducted using the diluted

ELISA diluent as shown in Fig. 10.

After incubation time was over, the plate was washed 4

times and then

100 μ L of each the standards and samples were pipetted to each were in technical duplicates and biological triplicates. Two wells containing 100 μ L of the *ELISA* diluent only were representative of blanks. The plate was then sealed and incubated at room temperature for 2 hours. Following the 2-hour incubation, the plate was washed thoroughly and then the detection antibody (250X) was diluted in the diluted *ELISA* diluent. Just as the capture

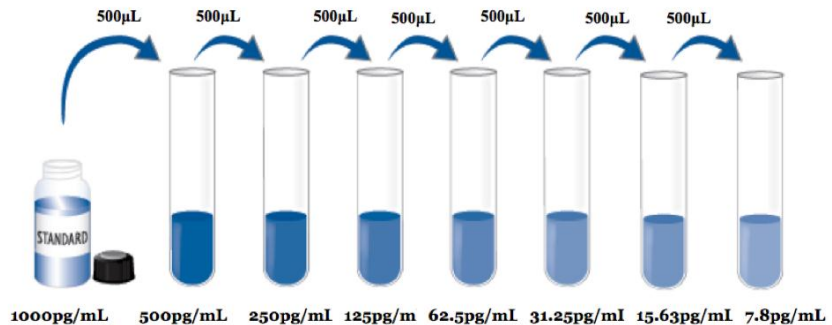


Figure 10 | Serial Dilutions of *ELISA* Standard

antibody, 100 μ L of the detection antibody was added to each well followed by an incubation at room temperature for 1 hour. After one hour, the plate was decanted and washed for 4 times. At this point, the 250X horseradish peroxidase (HRP) was diluted in the 1X *ELISA* diluent, whereby 100 μ L were added to each micro-well. The plate was then sealed and incubated for half an hour at room temperature. Finally, so as to detect the HRP, 100 μ L of 3,3',5,5'-tetramethylbenzidine (TMB) *ELISA* substrate was pipetted into each micro-well in the dark, after washing the plate thoroughly. The plate was then enfolded with aluminum foil and placed at room temperature for 30 minutes. In order to stop the assay, 50 μ L of the stop solution was pipetted to each well. The absorbance was read at a wavelength of 450nm using the spectrophotometer.

H. Statistical analyses

Data are represented as mean \pm SEM and all statistical tests were performed using GraphPad Prism 8 software. To determine whether there are any statistically significant differences between two experimental data sets, a non-paired student's t-test was performed. In analyzing significance, all *P*-values less than 0.05 were considered significant.

CHAPTER III

RESULTS

A. Differentiation of bone marrow-derived cells to macrophages

To isolate murine monocytes, bone marrows were isolated from the femurs and tibias of wild type C57BL/6 male mice. The extracted monocytes were then differentiated into macrophages by stimulation with L929 medium. Five days post-isolation, we used light microscopy to study the cells' morphology and examine their differentiation. Indeed, we observed spindle-shaped adherent cells in the Petri dishes reflecting the successful differentiation of monocytes to macrophages (Fig. 11 B) as compared to monocytes which are round cells in suspension (Fig. 11A).

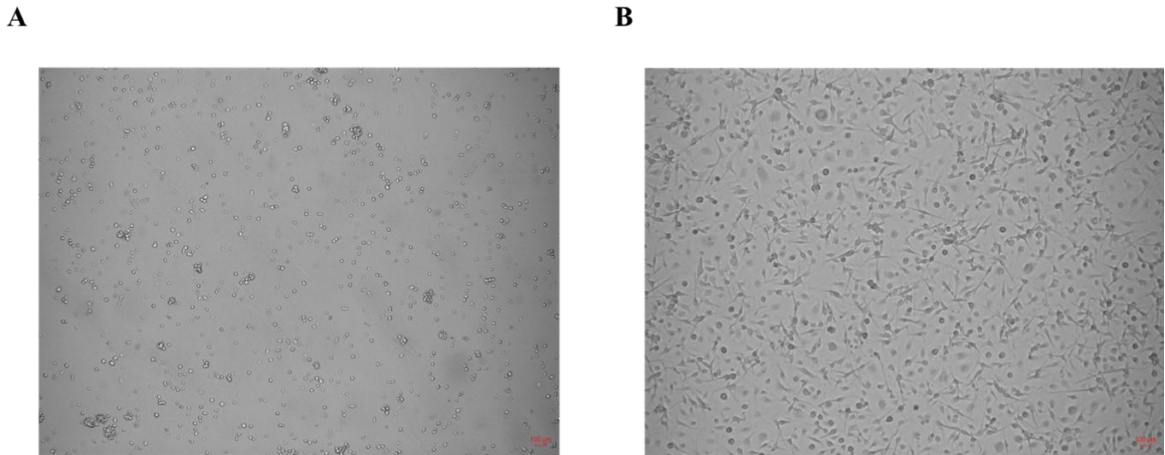


Figure 11 | Bone marrow-derived cells. (A) Isolated bone marrow-derived monocytes at day 0 of L929 stimulation. (B) Bone marrow-derived macrophages at day 6 of L929 stimulation.

B. Inflammatory effect of BK- and PK-stimulated macrophages

To evaluate the inflammatory effects of macrophages upon BK and PK treatment, BMDM cells were treated with PK (2.5 ng/mL), BK (10^{-7} M) and LPS (10 ng/mL) for 24 hours. After 24 hours, treatment was stopped, and media collected was subjected to *ELISA* in order to quantify IL-6 and TNF- α secretion. As shown in Fig.12 A and Fig.12 B, both BK and PK significantly up-regulated IL-6 and TNF- α production compared to the control, although to levels less than LPS.

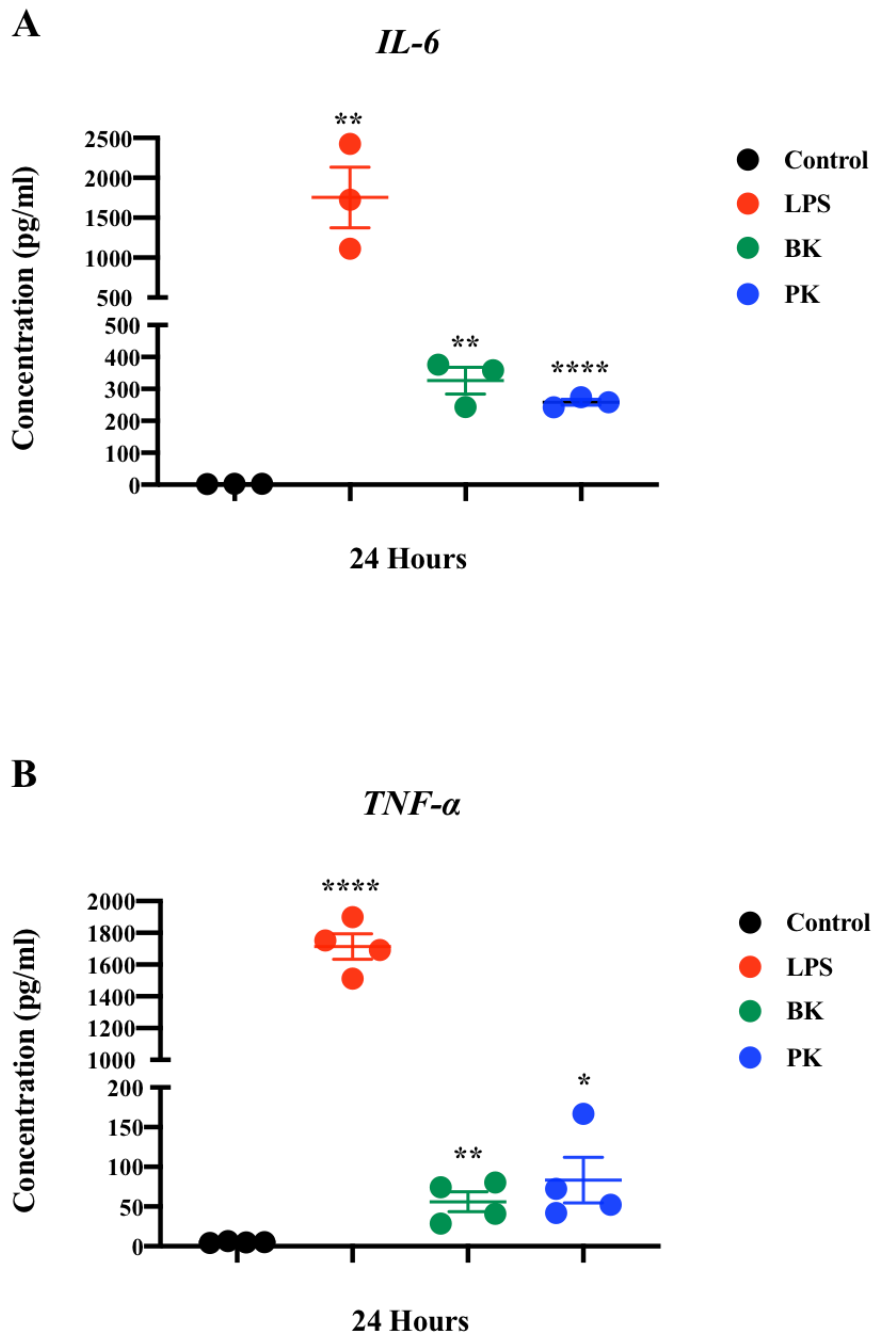
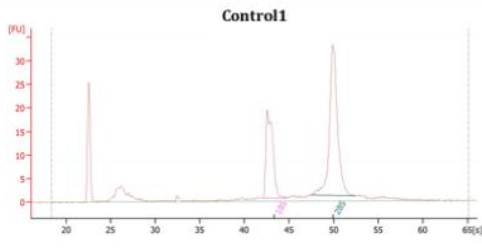


Figure 12 | Effect of Plasma Kallikrein and its mediator Bradykinin on Inflammatory Cytokines. Representative graph of (A) IL-6 and (B) TNF- α secretion by BMDM cells treated for 24 hours with 10 ng/mL LPS, 10^{-7} M BK and 2.5 ng/mL PK. Data are represented as mean \pm SEM (n=3), *P < 0.05; **P < 0.01; ****P < 0.0001 compared to the untreated control (Student's t-test).

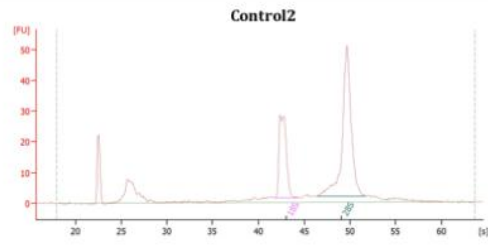
C. Stringent RNA Quality Control using Bioanalyzer

Prior to sequencing, the quality of each RNA was assessed using Bioanalyzer. There were four experimental groups of BMDM: control (untreated), LPS (positive control), BK and PK treated for 24 hours. The first peak shown in Fig. 13 is an internal standard. RNA Integrity Number reflects the quality of RNA and the surface area of the distinct peaks is used so as to calculate the RIN. The amount of the fluorescence is proportional to the size of RNA, thus the 28S peak is larger than the 18S peak. Being bigger in size, the 28S peak necessitates more time to migrate, hence it appears after the 18S peak on the electropherogram. Electropherograms revealed excellent profiles with high RNA Integrity Numbers (RIN). There was neither smearing nor any additional peaks evident, and the ribosomal RNA band 28S was about twice as big as the 18S band. Hence, RNA samples were considered to be good lacking any DNA contamination or degradation.

A

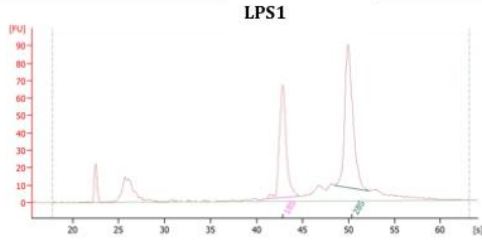
Overall Results for sample 1 : J1
 RNA Area: 169.7 RNA Integrity Number (RIN): 10 (8.02.09)
 RNA Concentration: 81 ng/ul Result Flagging Color:
 rRNA Ratio (28s / 18s): 1.8 Result Flagging Label: RIN: 10

Fragment table for sample 1 : J1				
Name	Start Time [s]	End Time [s]	Area	% of total Area
18S	41.99	44.81	37.9	22.4
28S	47.45	52.45	67.7	39.9

B

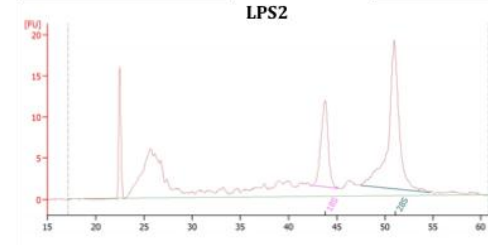
Overall Results for sample 9 : J9
 RNA Area: 290.6 RNA Integrity Number (RIN): 9.7 (8.02.09)
 RNA Concentration: 139 ng/ul Result Flagging Color:
 rRNA Ratio (28s / 18s): 1.9 Result Flagging Label: RIN: 9.70

Fragment table for sample 9 : J9				
Name	Start Time [s]	End Time [s]	Area	% of total Area
18S	41.77	44.35	59.1	20.3
28S	46.43	51.69	112.6	38.8

C

Overall Results for sample 6 : J6
 RNA Area: 558.9 RNA Integrity Number (RIN): 10 (8.02.09)
 RNA Concentration: 268 ng/ul Result Flagging Color:
 rRNA Ratio (28s / 18s): 1.3 Result Flagging Label: RIN: 10

Fragment table for sample 6 : J6				
Name	Start Time [s]	End Time [s]	Area	% of total Area
18S	41.07	44.68	132.5	23.7
28S	48.48	52.23	170.0	30.4

D

Overall Results for sample 2 : J1
 RNA Area: 196.7 RNA Integrity Number (RIN): 8.4 (8.02.09)
 RNA Concentration: 141 ng/ul Result Flagging Color:
 rRNA Ratio (28s / 18s): 2.2 Result Flagging Label: RIN: 8.40

Fragment table for sample 2 : J1				
Name	Start Time [s]	End Time [s]	Area	% of total Area
18S	42.49	45.22	20.9	10.6
28S	47.51	54.73	46.0	23.4

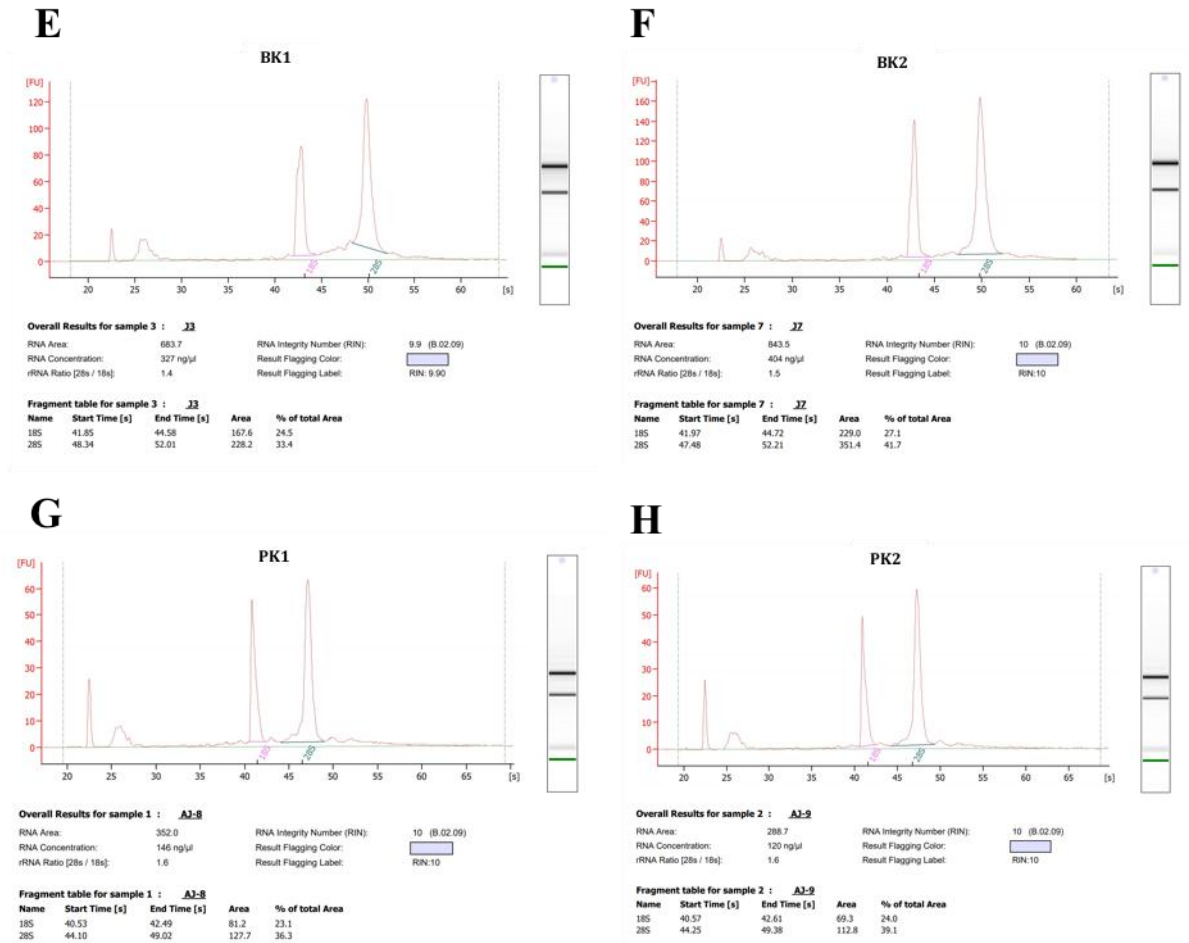


Figure 13 | Bioanalyzer Electropherogram Profile for 8 RNA Samples (Control, LPS, BK and PK). Electropherograms portray fluorescence intensity versus migration time on the y-axis and x-axis, respectively. Electropherograms for (A, B) control, (C, D) LPS, (E, F) BK and (G, H) PK BMDM RNAs.

D. RNA-seq Data Processing

Duplicates of each sample were sent for RNA-sequencing which was conducted in the Pillar Genomics Institute of Precision Medicine at AUBMC. After sequencing was carried out, data was processed using the DESeq2 tool using bam files of individual samples in the Galaxy platform. Correlograms were conducted in order to assess the magnitude of variability between the different experimental groups. The dendrogram on Fig. 14 demonstrates the magnitude of similarity between samples. Knowing that the shorter the dendrogram arm is, the more similar samples are, our duplicates demonstrate high levels of association. Another way to determine sample-to-sample distances, based on their overall gene expression, is Principal Component Analysis (PCA). Data points (samples) are projected onto the 2D plane such that they spread out in the two directions that elucidate most of the variances (Fig. 15). The samples are separated according to two principal components, PC1 and PC2, whereby they represent factors lying behind the variances observed. The transcriptomes of BMDM samples in the individual datasets must be different from each other since they were exposed to distinct treatments. For example, all the treated samples were located far from the controls in the gene expression PCA plot, hence suggesting that the treated samples are distinct to the untreated ones. Furthermore, in terms of gene expression profiles, the closer the duplicates emerge on the PCA plot, the more alike they are as seen in Fig. 15. So as to look at the pattern of gene expression, MA plots were generated (Fig. 16). The plot demonstrates the variances between measurements after transforming the raw data onto M (log ratio) and A (mean average) scales. The scatter plot shows the Log₂ fold change on the y-axis versus the mean expression of normalized

counts for a given sample on the x-axis. Genes with an adjusted p-value less than 0.05 are represented in red.

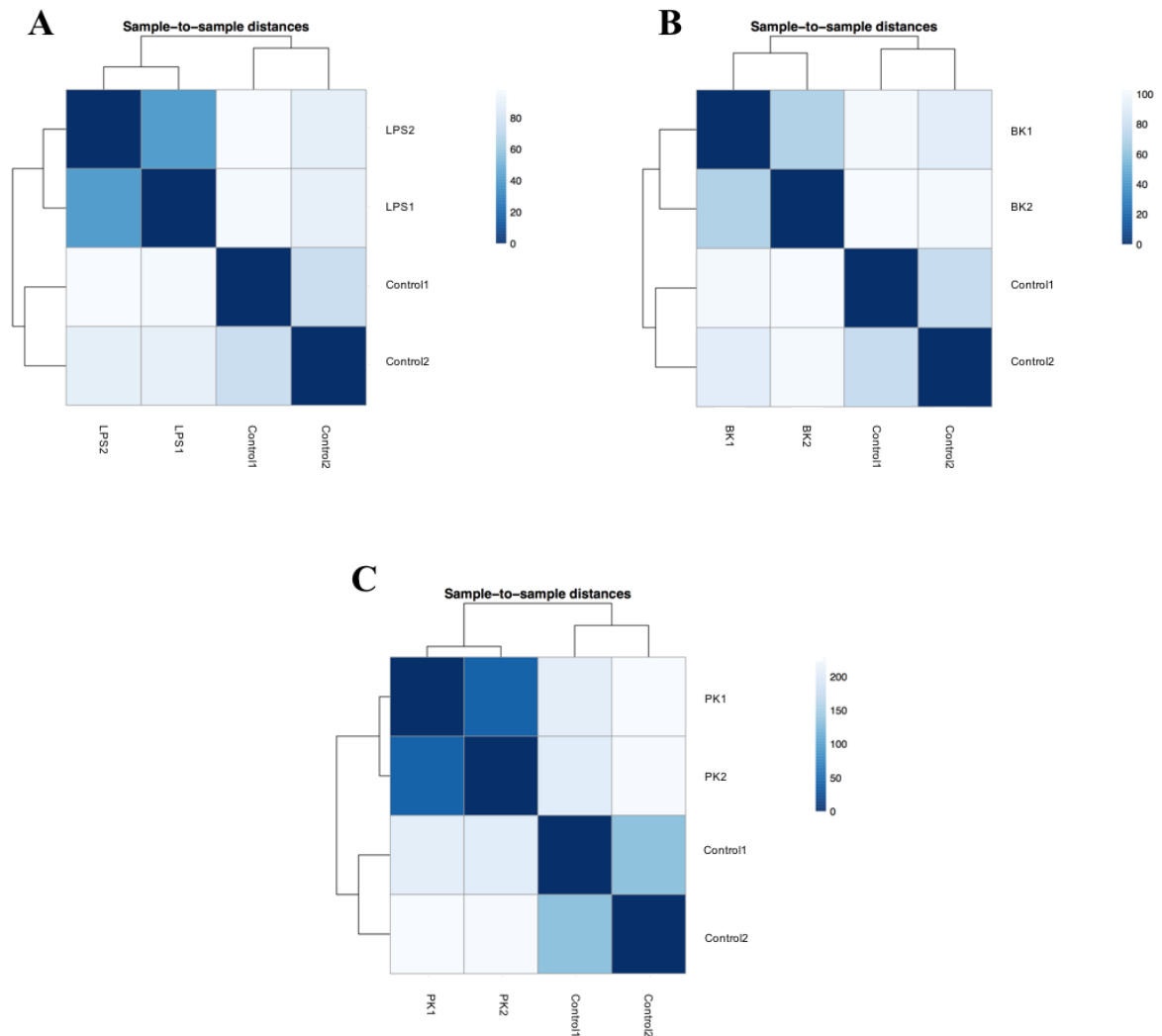


Figure 14 | Correlation Matrix on Aligned Reads. Spearman correlation on aligned reads visualizing the correlation between samples. Correlation matrix was generated using the DESeq2 tool. Correlogram for (A) LPS, (B) BK and (C) PK treated BMDM RNA samples. Scale bar represents the range of the correlation coefficients displayed.

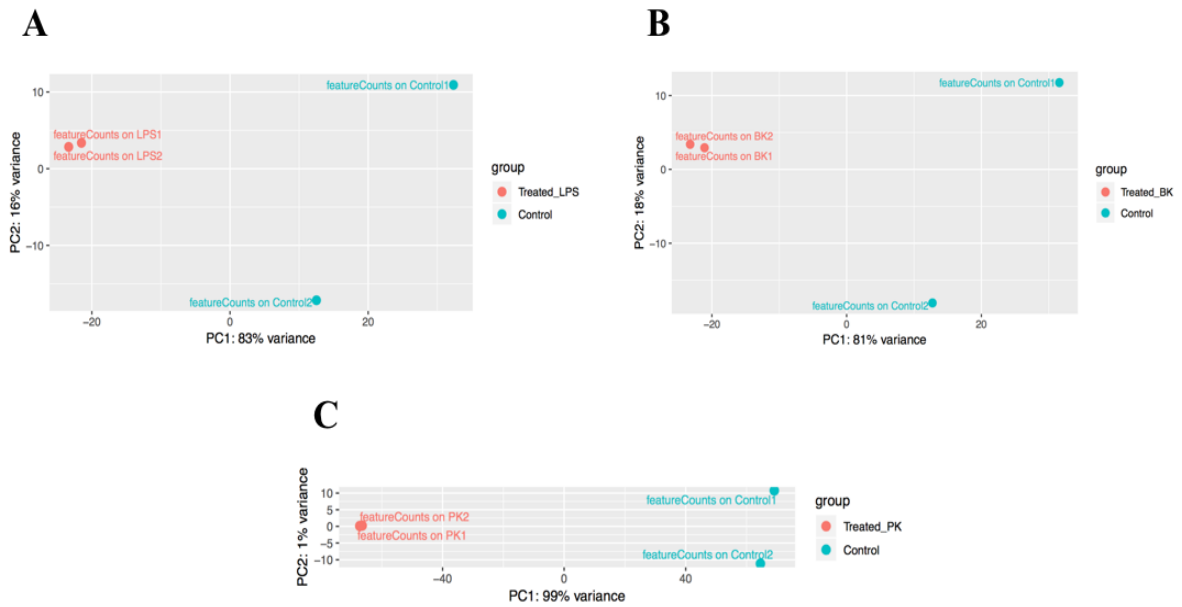


Figure 15 | Principal Component Analysis Plot. PCA plots of RNA-seq data assessing inter and intragroup variability displaying (A) LPS, (B) BK, (C) and PK treated BMDM RNA samples as opposed to controls. Each dot indicates a sample where treatments are given their own color.

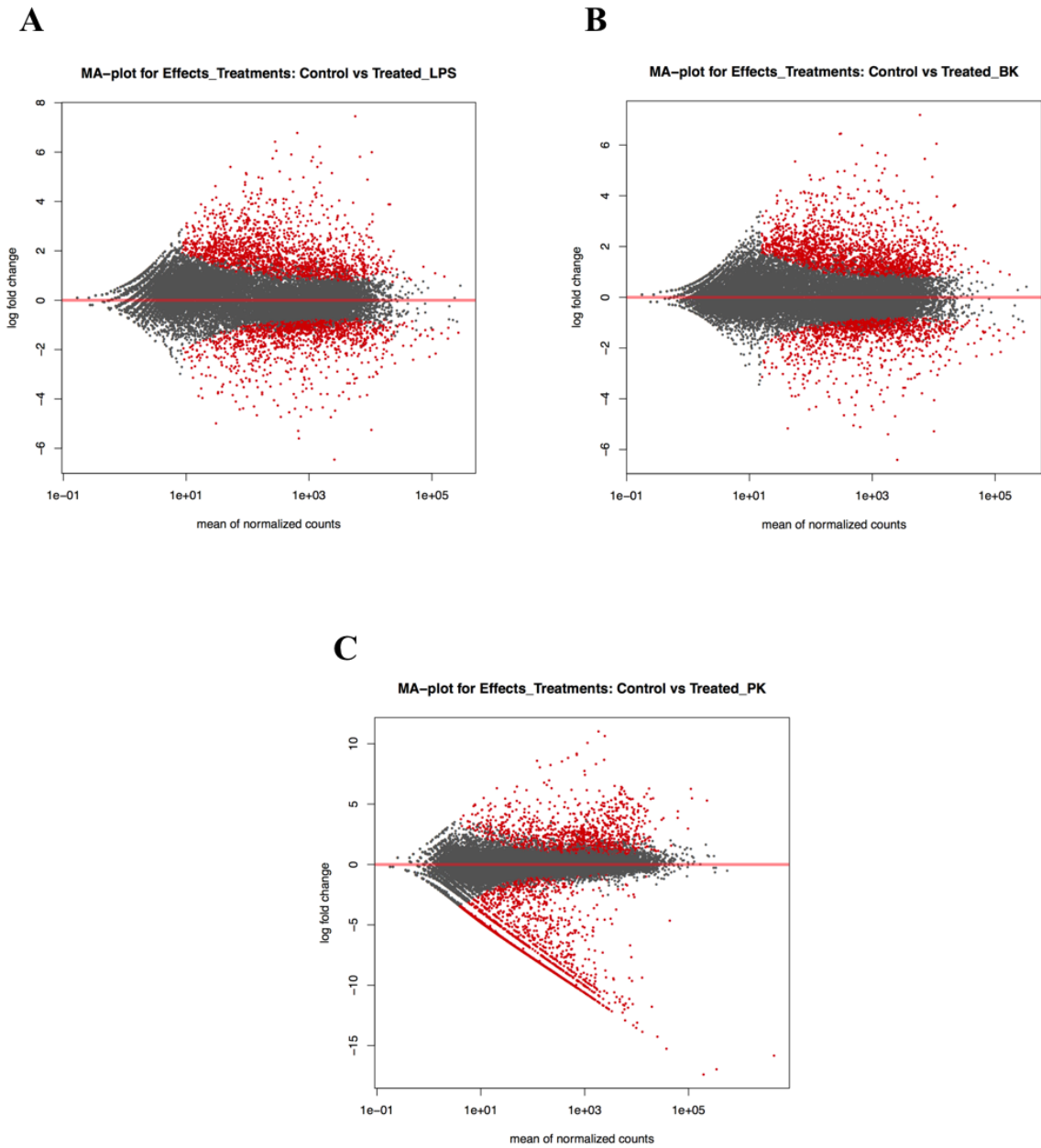


Figure 16 | MA plot. MA plot for differential expression analysis in (A) LPS, (B) BK and (C) PK treated BMDM RNA samples. The circles represent different genes, whereby the red color indicates the most significant differentially expressed observation. The y-axis indicates the Log₂ fold change and the x-axis indicates the normalized mean.

E. Clustering of the Expressed Genes via Heatmap

Using the data generated from RNA-seq, a heatmap was constructed for four experimental groups demonstrating the clustering of regulated genes. Each row represents the relative expression level of a single gene whereas each column shows the expression level of a single sample. The dendrogram on the top of Fig 17 shows how the untreated control samples, LPS- and BK-treated samples are clustered together at a distance from PK-stimulated sample. This indicates that PK has a different expression profile than the rest of the groups.

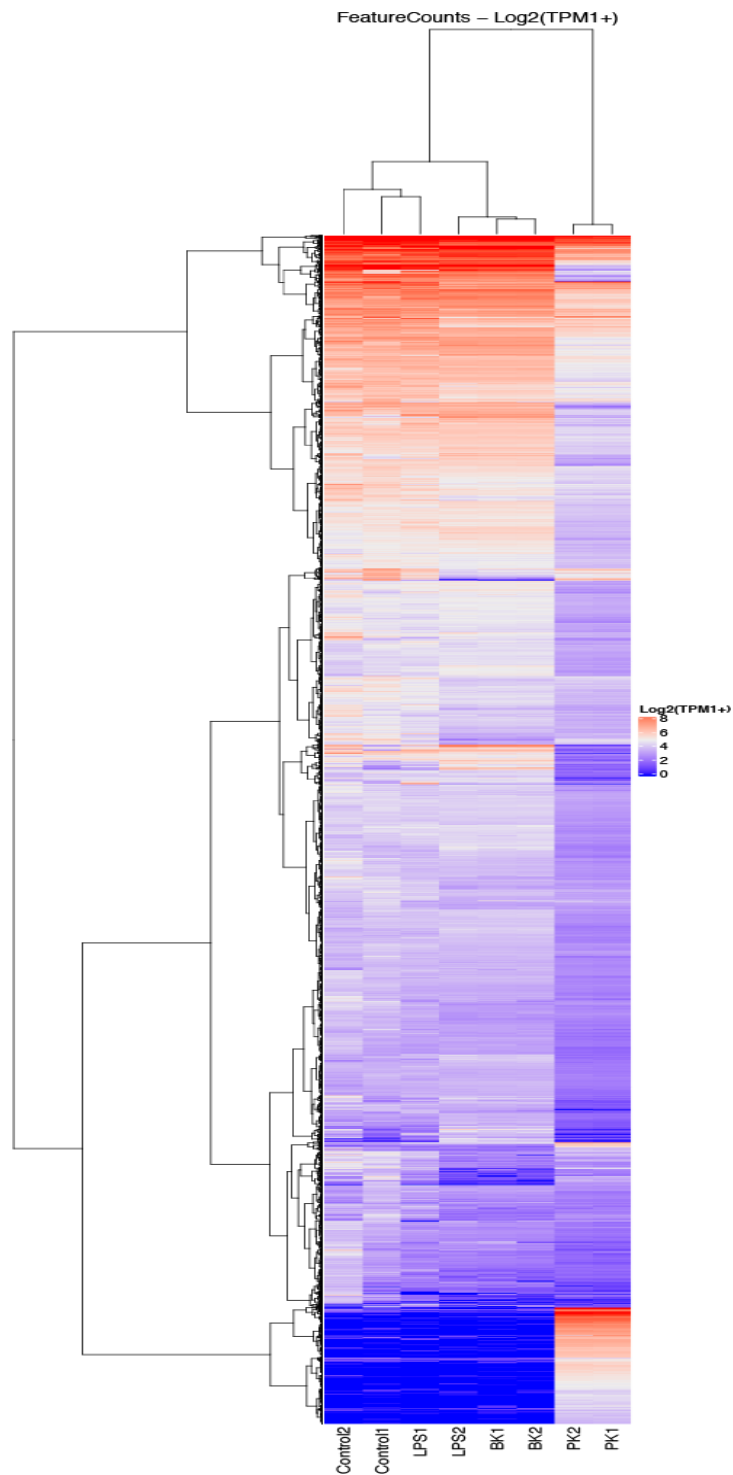


Figure 17 | Genome-wide transcriptome heatmap analysis of RNA-Seq derived gene expression data. Unsupervised hierarchical clustering was applied on genes and samples represented as rows and columns, respectively. Same Log2(TPM+1) scale was applied.

F. Investigation of the Transcriptomic Data

RNA-sequencing analysis showed around 55,000 regulated genes. However, this number was decreased significantly when applying a Log₂ fold change of ± 1 and a p-adjusted < 0.05 . The pattern of up-regulated and down-regulated genes in the experimental groups is depicted in Table 2 and Fig. 18 below:

Table 2 | The variation in the regulated gene numbers in the three treated groups.

Condition	Number of Up-regulated Genes	Number of Down-regulated Genes
Control vs. LPS	1345	921
Control vs. BK	1531	856
Control vs. PK	997	1932

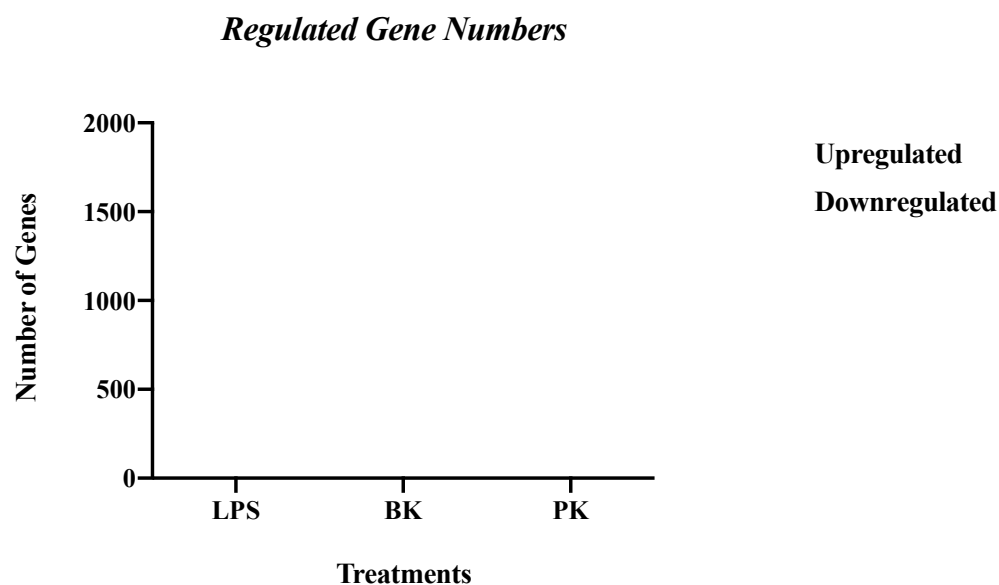


Figure 18 | Bar graph depicting the number of regulated genes in three experimental groups. Red and blue bars indicate the number of up-regulated and down-regulated genes, respectively.

G. Differential Gene Expression

A set of inflammatory, fibrotic as well as oxidative stress genes having a p-value and p-adjusted less than 0.05 were selected after adjusting the Log2 fold change for less than -1 representing down-regulated genes and greater than +1 representing up-regulated genes. Each gene along its Log2 fold change, fold change, p-value and p-adjusted are illustrated in the Tables 3, 4 and 5.

Table 3 | Comparative list of genes in LPS-stimulated BMDMs for 24 hours compared to control.

Gene Name	Log2 Fold Change	Fold Change	P-Value	P-Adjusted
Ccl6	3.347	10.177	0.000	0.000
Ccl9	2.541	5.819	0.000	0.000
Ccn4	1.867	3.648	0.006	0.043
Ccr2	3.773	13.671	0.000	0.000
Ccr3	2.007	4.018	0.000	0.005
Ccr5	1.483	2.795	0.001	0.011
Cd163	4.524	23.002	0.000	0.000
Cd177	2.292	4.896	0.001	0.007
Cd200r1	1.645	3.127	0.002	0.016
Cd209f	2.719	6.582	0.001	0.009
Cd28	1.996	3.989	0.000	0.005
Cd300ld3	1.882	3.687	0.000	0.000
Cd55	3.145	8.846	0.000	0.000
Cd55b	3.623	12.319	0.000	0.000
Cd74	2.046	4.129	0.000	0.002
Cd79b	3.662	12.655	0.000	0.000
Cd81	1.676	3.195	0.000	0.006
Cd83	1.549	2.926	0.000	0.004
Cd93	1.836	3.570	0.000	0.002
Fgf11	3.990	15.890	0.000	0.000
Fgf13	2.577	5.965	0.000	0.002
Fn1	1.948	3.859	0.003	0.025
Igf1r	1.903	3.740	0.000	0.000
Igf2bp3	1.204	2.304	0.003	0.024
Il10	1.548	2.925	0.000	0.002
Il16	1.716	3.285	0.000	0.000
Il18rap	3.401	10.562	0.000	0.000
Il1r2	2.464	5.516	0.000	0.003
Il1rl1	2.283	4.866	0.004	0.030
Il21r	1.289	2.444	0.000	0.002
Il2ra	2.062	4.176	0.001	0.007
Il6ra	1.583	2.996	0.000	0.000
Itga1	2.061	4.173	0.001	0.014
Itga4	1.405	2.648	0.000	0.000

Itga6	1.374	2.592	0.003	0.026
Itga8	2.685	6.432	0.000	0.000
Itga9	3.362	10.281	0.000	0.000
Itgal	2.017	4.047	0.000	0.003
Itgax	2.338	5.055	0.000	0.006
Itgb2l	3.532	11.569	0.000	0.000
Itgb5	1.131	2.190	0.004	0.033
Nos1ap	3.313	9.941	0.000	0.000
Nox1	1.252	2.381	0.002	0.020
Ptger3	1.797	3.475	0.006	0.042
Ptgs1	3.078	8.446	0.000	0.000
Tgfbr2	1.356	2.560	0.000	0.003
Tgfbr3	2.142	4.415	0.000	0.003
Tnfrsf11a	1.355	2.557	0.000	0.004
Tnfsf14	2.159	4.466	0.001	0.010
Ccl2	-2.150	0.225	0.000	0.000
Ccl8	-1.856	0.276	0.000	0.001
Cd109	-1.571	0.337	0.001	0.009
Cd1d1	-3.000	0.125	0.000	0.000
Cd200	-4.337	0.049	0.000	0.000
Cd244a	-1.171	0.444	0.000	0.003
Cd24a	-4.709	0.038	0.000	0.000
Cd274	-1.572	0.336	0.004	0.030
Cd276	-1.705	0.307	0.000	0.006
Cd300lf	-3.409	0.094	0.000	0.000
Col15a1	-2.575	0.168	0.000	0.000
Col27a1	-2.936	0.131	0.000	0.000
Colgalt1	-1.052	0.482	0.002	0.023
Cxcl1	-2.228	0.213	0.000	0.005
Cxcl11	-3.496	0.089	0.000	0.000
Cxcl16	-1.367	0.388	0.000	0.000
Cxcl2	-1.982	0.253	0.001	0.012
Cxcl9	-3.309	0.101	0.000	0.000
Cxcr4	-1.429	0.371	0.001	0.007
Cxxc1	-1.162	0.447	0.000	0.006
Il18bp	-1.597	0.331	0.000	0.001
Il1f6	-2.613	0.163	0.000	0.002
Il1f9	-2.657	0.158	0.000	0.000

Il1r1	-2.545	0.171	0.000	0.000
Il1r2	-3.801	0.072	0.000	0.000
Il1rn	-1.812	0.285	0.000	0.000
Il7	-1.599	0.330	0.006	0.047
Il7r	-2.978	0.127	0.000	0.000
Lgals3bp	-1.368	0.388	0.000	0.001
Tuba4a	-1.590	0.332	0.000	0.000

Table 4 | Comparative list of genes in BK-stimulated BMDMs for 24 hours compared to control.

Gene Name	Log2 Fold Change	Fold Change	P-Value	P-Adjusted
Ccl6	3.148	8.862	0.000	0.000
Ccl9	2.426	5.375	0.000	0.000
Cd160	1.063	2.089	0.006	0.043
Cd163	4.017	16.190	0.000	0.000
Cd177	2.273	4.834	0.001	0.013
Cd200r1	1.503	2.834	0.002	0.021
Cd207	2.711	6.548	0.001	0.008
Cd28	1.869	3.654	0.000	0.005
Cd300ld3	1.595	3.021	0.000	0.003
Cd5	1.560	2.948	0.006	0.039
Cd55	2.967	7.817	0.000	0.000
Cd55b	2.609	6.101	0.000	0.005
Cd74	1.945	3.851	0.000	0.002
Cd79b	3.440	10.853	0.000	0.000
Cd81	1.544	2.916	0.001	0.010
Cd83	1.692	3.231	0.000	0.001
Cd93	1.620	3.073	0.000	0.003
Col10a1	1.584	2.999	0.001	0.009
Cx3cl1	2.382	5.214	0.001	0.009
Fgf11	3.479	11.147	0.000	0.000
Il10	1.639	3.114	0.000	0.000
Il15	1.300	2.462	0.002	0.015
Il16	1.533	2.894	0.000	0.001
Il18rap	2.733	6.646	0.000	0.000
Il21r	1.284	2.436	0.000	0.005
Il6ra	1.692	3.232	0.000	0.000
Lgals1	1.395	2.630	0.001	0.014
Mmp9	1.640	3.117	0.001	0.007
Nos1ap	3.223	9.335	0.000	0.000
Nox1	1.194	2.288	0.005	0.034
Ptgs1	2.693	6.468	0.000	0.000
Tnfrsf11a	1.417	2.671	0.000	0.001
Tnfsf14	2.351	5.101	0.001	0.008
Col15a1	-2.421	0.187	0.000	0.000

Col27a1	-2.633	0.161	0.000	0.000
Il18bp	-1.698	0.308	0.000	0.000
Il1f6	-2.359	0.195	0.001	0.009
Il1f9	-2.573	0.168	0.000	0.000
Il1r1	-2.378	0.192	0.000	0.000
Il1rl2	-3.693	0.077	0.000	0.000
Il1rn	-1.591	0.332	0.000	0.001
Il7r	-2.830	0.141	0.000	0.000
Ptger2	-1.686	0.311	0.000	0.001
Ptges2	-1.057	0.481	0.006	0.042
Ptgir	-1.341	0.395	0.004	0.032
Ptgr1	-1.629	0.323	0.000	0.000
Tuba4a	-1.573	0.336	0.000	0.000

Table 5 | Comparative list of genes in PK-stimulated BMDMs for 24 hours compared to control.

Gene Name	Log2 Fold Change	Fold Change	P-Value	P-Adjusted
Ccl5	6.229	75.024	0.000	0.000
Ccl8	2.454	5.477	0.000	0.002
Ccr7	2.805	6.989	0.000	0.001
Ccr9	1.897	3.725	0.001	0.012
Ccr12	3.803	13.953	0.000	0.002
Cd209c	5.115	34.645	0.000	0.000
Cd300ld4	2.737	6.665	0.001	0.011
Cd63	3.313	9.935	0.000	0.000
Cxcl1	4.458	21.984	0.000	0.000
Cxcl10	2.705	6.520	0.003	0.025
Cxcl11	3.945	15.401	0.002	0.016
Cxcl2	4.617	24.531	0.000	0.000
Cxcl3	3.952	15.471	0.001	0.008
Edn1	2.907	7.502	0.003	0.033
Il12b	3.346	10.165	0.000	0.003
Il1a	5.192	36.562	0.000	0.000
Il1b	3.276	9.684	0.000	0.000
Il1bos	4.756	27.026	0.000	0.000
Il1f6	3.699	12.983	0.003	0.025
Il20rb	1.224	2.336	0.001	0.010
Il23r	3.953	15.487	0.000	0.000
Il6	3.743	13.385	0.000	0.000
Il7	2.675	6.387	0.004	0.034
Mif	3.645	12.511	0.000	0.000
Nos2	5.101	34.318	0.000	0.000
Ptges	4.381	20.832	0.000	0.001
Ptges3	1.872	3.661	0.000	0.000
Ptgs2	5.446	43.595	0.000	0.000
Ptgs2os2	3.202	9.200	0.002	0.024
Romo1	1.677	3.199	0.000	0.000
Tnf	2.953	7.743	0.003	0.033
Tnfrsf8	3.519	11.467	0.001	0.010
Fn1	-1.809	0.285	0.003	0.025

Il2ra	-2.199	0.218	0.006	0.050
Il31ra	-3.698	0.077	0.000	0.001
Mmp9	-1.724	0.303	0.000	0.001
Tubb2a-ps2	-5.932	0.016	0.000	0.000
Tubb4b-ps1	-8.950	0.002	0.000	0.000
Tubb4b-ps2	-4.276	0.052	0.000	0.002

H. Investigation of the Comparative Gene Expression via Venn Diagram

Using Venny software, Venn diagrams were constructed so as to facilitate the analysis of the distinct genes expressed in the different groups. The distribution of the number of genes between the three sets of conditions are shown in individual diagrams in figure 19, whereas the overlapping parts of the diagrams demonstrate the common genes present in the corresponding experimental groups. Although 465 up-regulated genes were identified to be common between LPS- and BK-treated samples, only 2 genes were found to be shared between LPS- and PK-treated samples as well as between BK- and PK-stimulated ones.

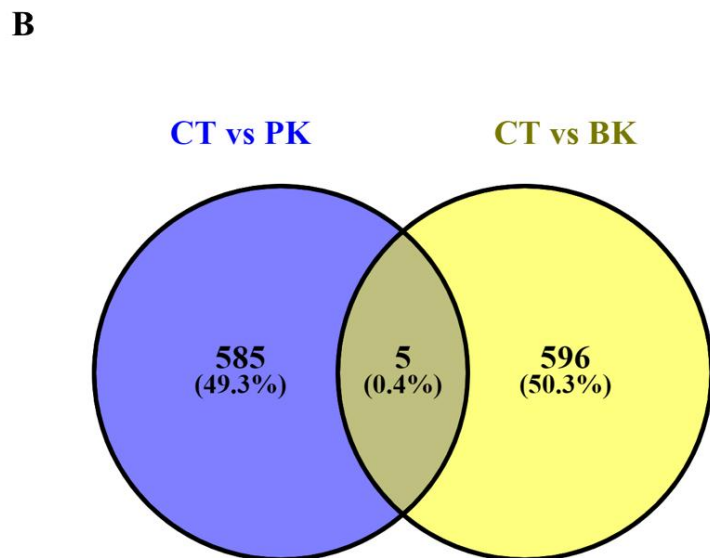
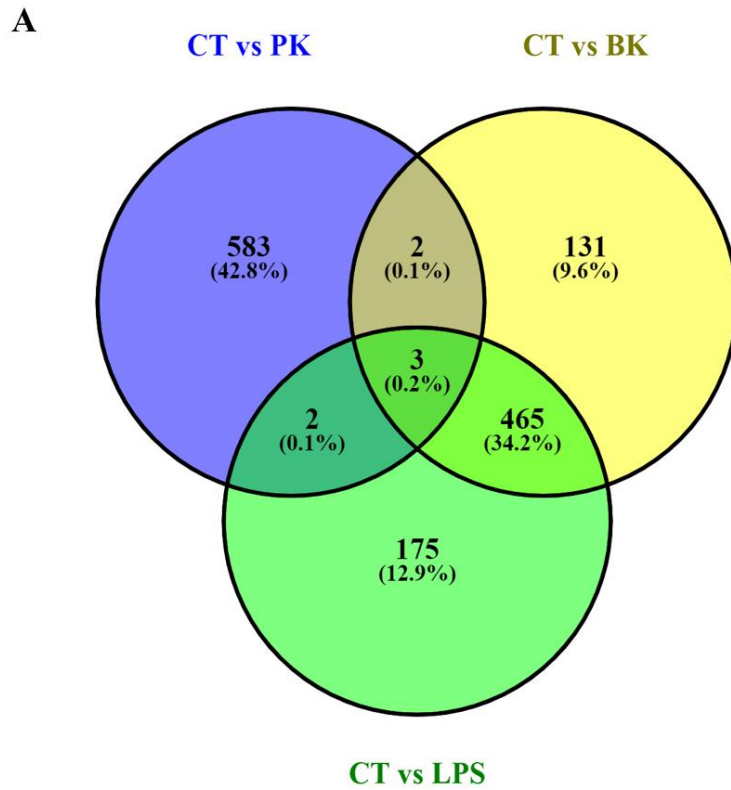


Figure 19 | Venn diagram. Venn diagram demonstrating the appearance of common genes between (A) the different groups; LPS-, BK- and PK-treated BMDMs and (B) BK- and PK-treated BMDMs versus controls.

I. Identification of Altered Pathways

Using PANTHER (Protein ANalysis THrough Evolutionary Relationships), genes in PK-stimulated BMDM cells were classified into several groups depending on their biological process, in order to facilitate high-throughput analysis. The PANTHER classifications are the result of human curation as well as sophisticated bioinformatics algorithms (Thomas, Campbell et al. 2003). Lists of pathways in LPS-, BK- and PK-treated BMDMs were retrieved indicating the percentage of proteins altered in each pathway represented in Table 6 and Fig. 20, Table 7 and Figure 21, and Table 8 and Figure 22, respectively.

Table 6 | List of Altered Pathways in Response to LPS Stimulation

Statistically Significant Altered Pathways	Number of Proteins	Percentage of Protein Hit Against Total # Proteins
Developmental Process	32	6.40%
Multicellular Organismal Process	34	6.80%
Cellular Process	197	39.20%
Reproduction	7	1.40%
Cell Population Proliferation	3	0.60%
Localization	64	12.70%
Reproductive Process	7	1.40%
Multi-Organism Process	19	3.80%
Biological Adhesion	8	1.60%
Immune System Process	25	5.00%
Cellular Component Organization or Biogenesis	71	14.10%
Biological Regulation	142	28.30%
Growth	2	0.40%
Signaling	81	16.10%
Metabolic Process	102	20.30%
Response to Stimulus	99	19.70%
Biom mineralization	2	0.40%
Biological Phase	2	0.40%
Behavior	1	0.20%
Locomotion	16	3.20%

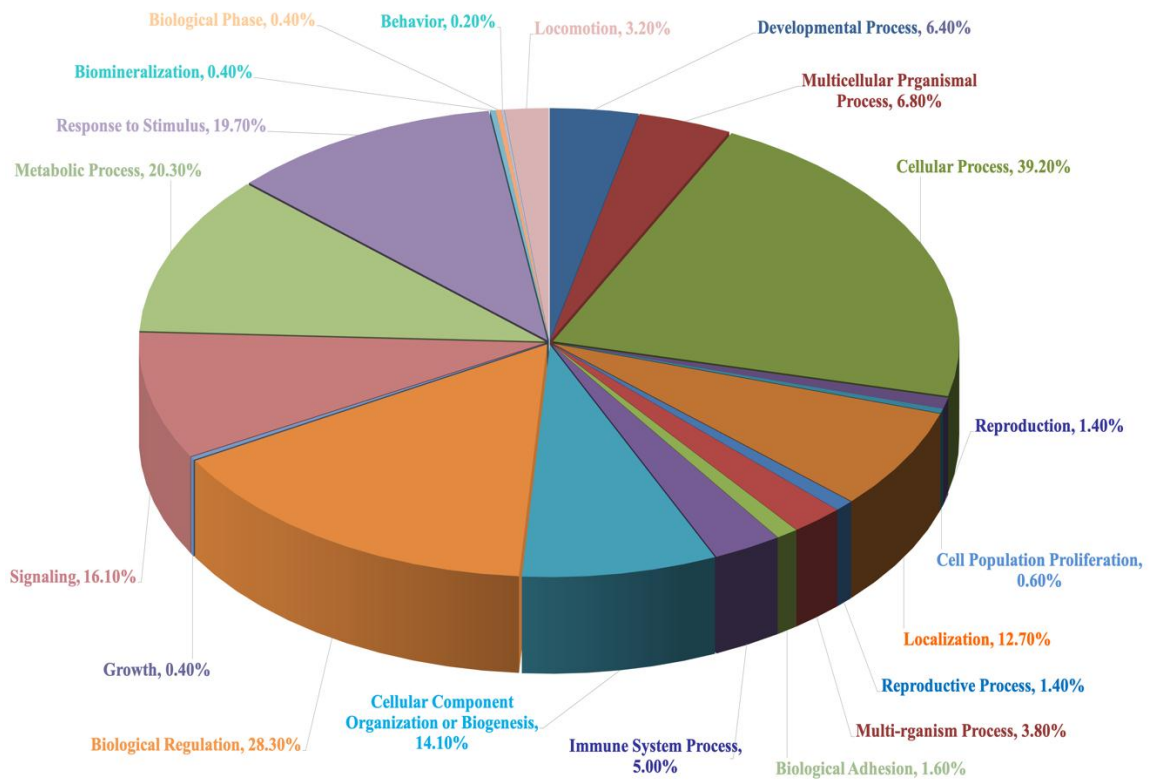


Figure 20 | Pie Chart. Distinct altered pathways in macrophages in response to LPS stimulation showing the percentages of proteins hit in each pathway.

Table 7 | List of Altered Pathways in Response to BK Stimulation

Statistically Significant Altered Pathways	Number of Proteins	Percentage of Protein Hit Against Total # Proteins
Developmental Process	24	5.40%
Multicellular Organismal Process	23	5.10%
Cellular Process	171	38.30%
Reproduction	8	1.80%
Cell Population Proliferation	3	0.70%
Localization	53	11.90%
Reproductive Process	8	1.80%
Multi-Organism Process	15	3.40%
Biological Adhesion	5	1.10%
Immune System Process	20	4.50%
Cellular Component Organization or Biogenesis	56	12.50%
Biological Regulation	127	28.40%
Signaling	69	15.40%
Metabolic Process	90	20.10%
Response to Stimulus	83	18.60%
Biom mineralization	2	0.40%
Biological Phase	2	0.40%
Locomotion	14	3.10%

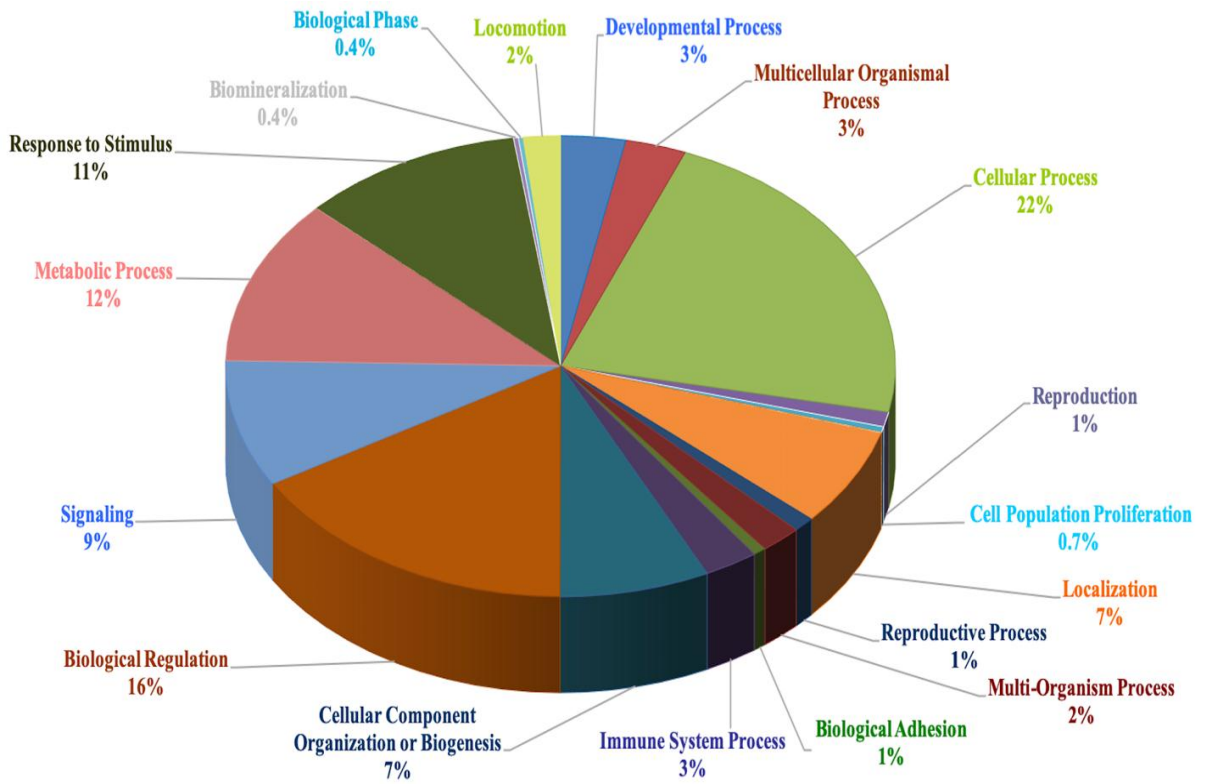


Figure 21 | Pie Chart. Distinct altered pathways in macrophages in response to BK stimulation showing the percentages of proteins hit in each pathway.

Table 8 | List of Altered Pathways in Response to PK stimulation.

Statistically Significant Altered Pathways	Number of Proteins	Percentage of Proteins Hit Against Total Number of Proteins
Cellular Component Organization or Biogenesis	21	5.10%
Cellular Process	121	29.20%
Localization	45	10.80%
Reproduction	1	0.20%
Biological Regulation	57	13.70%
Response to Stimulus	51	12.30%
Developmental Process	3	0.70%
Rhythmic Process	1	0.20%
Multicellular Organismal Process	19	4.60%
Biological Adhesion	7	1.70%
Metabolic Process	110	26.50%
Cell Proliferation	2	0.50%
Immune System Process	31	7.50%

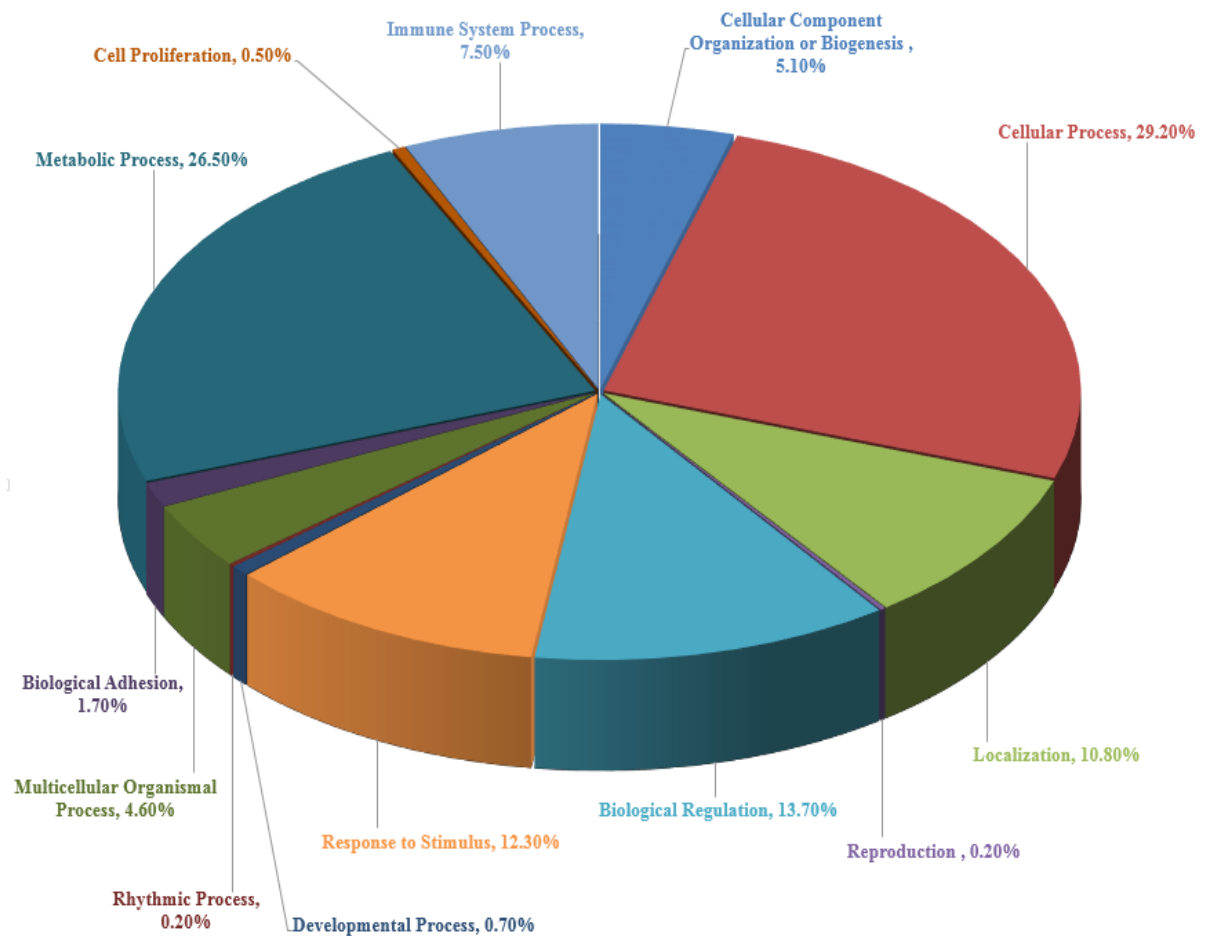


Figure 22| Pie Chart. Distinct altered pathways in macrophages in response to PK stimulation showing the percentages of proteins hit in each pathway.

J. Validation of the Transcriptomic Data *via* RT-qPCR

We next assessed the gene expression of inflammatory and anti-inflammatory markers by RT-qPCR. Fig. 23 illustrates that PK-treated macrophages showed a significant increase in IL-6, TNF- α , Gal-3 and iNOS gene expression compared to the untreated controls for 24 hours. No significant effect was shown on the expression of IL-1 β , CCL2 and MMP-9 (Fig. 23).

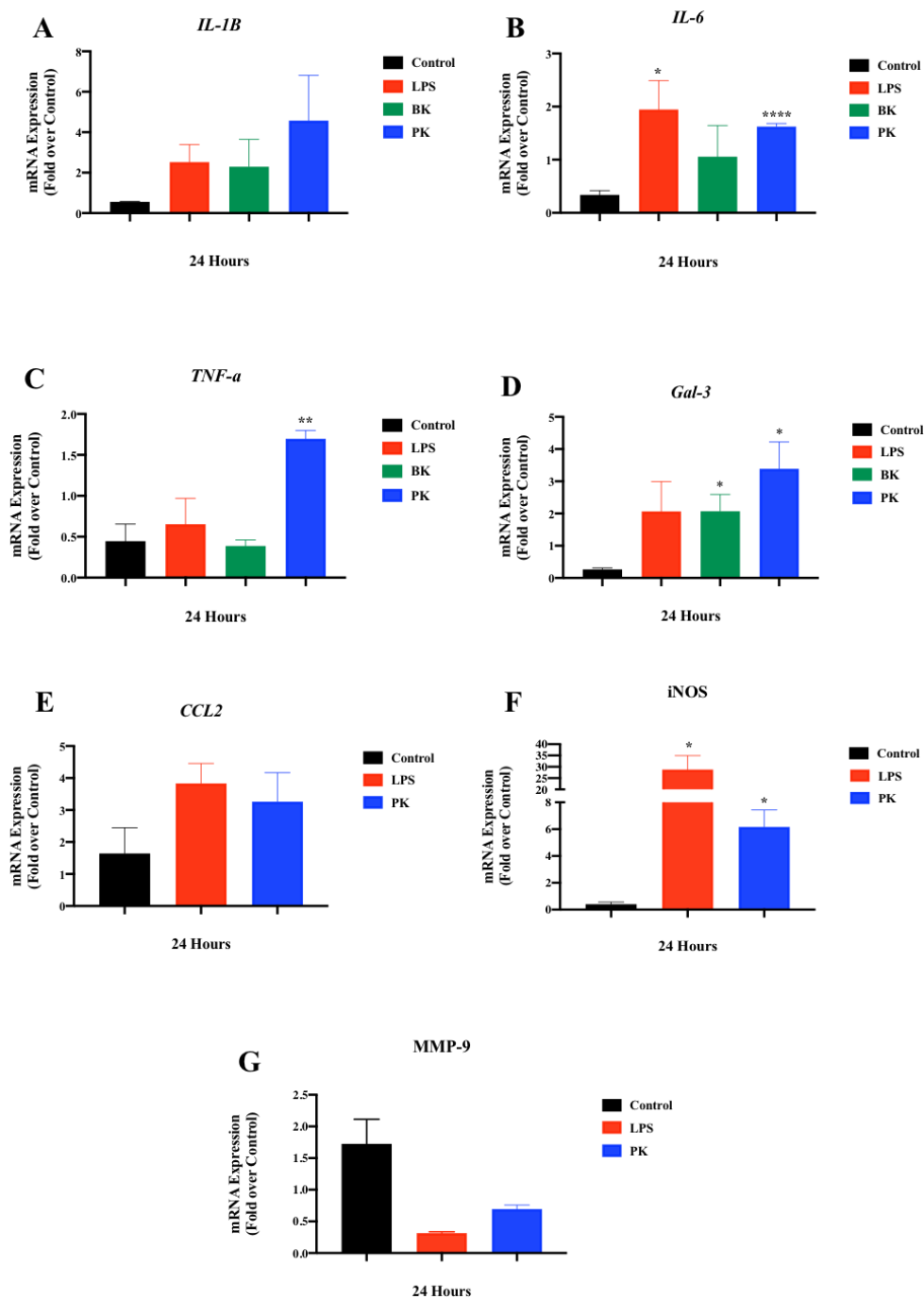
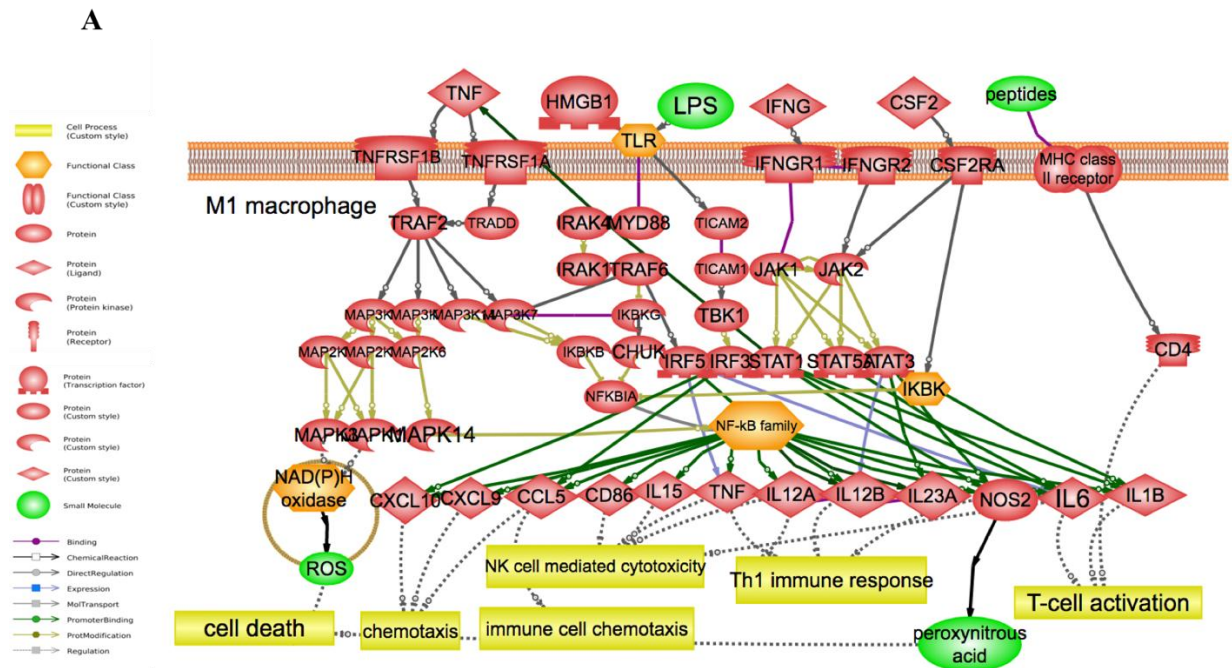
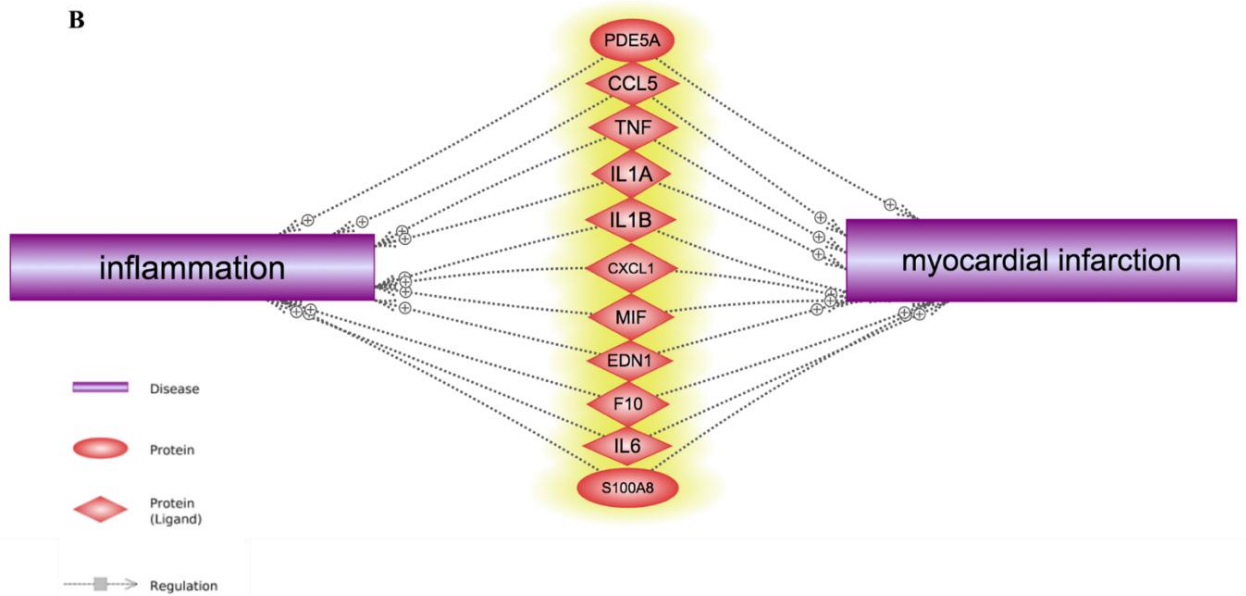
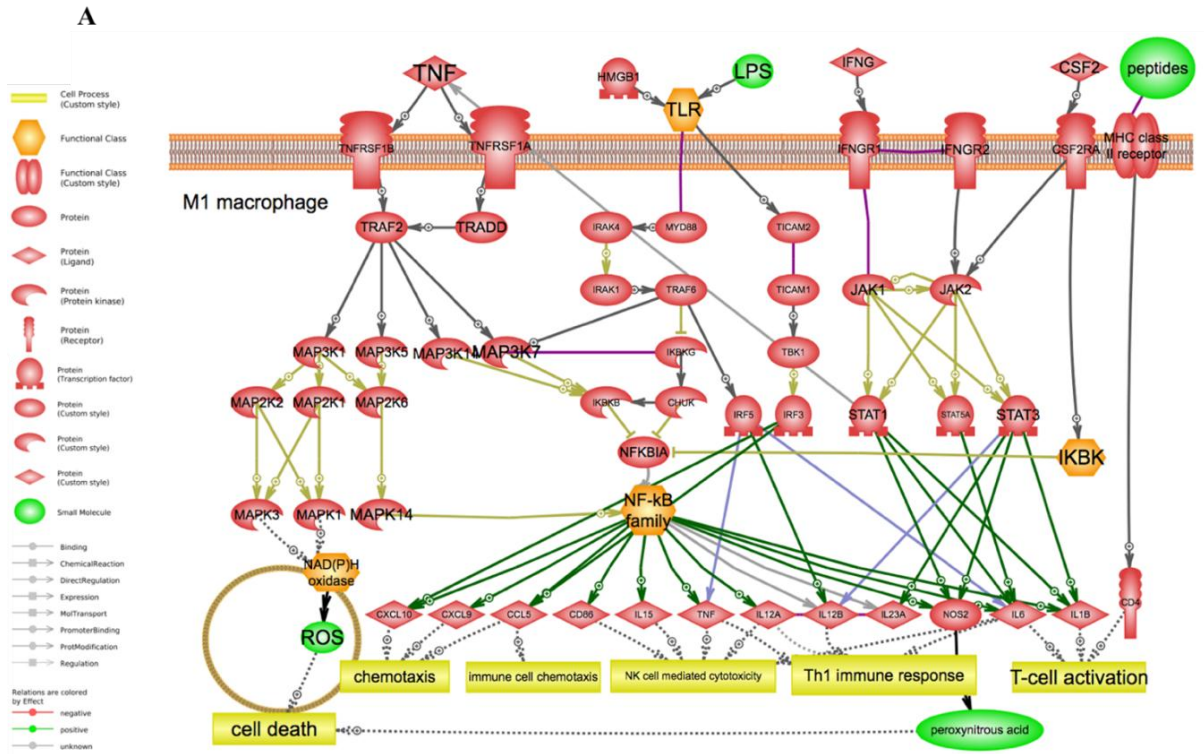


Figure 23 | Effect of Plasma Kallikrein and Bradykinin on Gene Expression. Representative graph of gene expression of (A) IL-1 β , (B) IL-6, (C) TNF- α , (D) Gal-3, (E) CCL2, (F) iNOS and (G) MMP-9. Data are represented as mean \pm SEM (n=3), *P < 0.05; **P < 0.01; ****P < 0.0001 compared to the untreated control (Student's t-test).

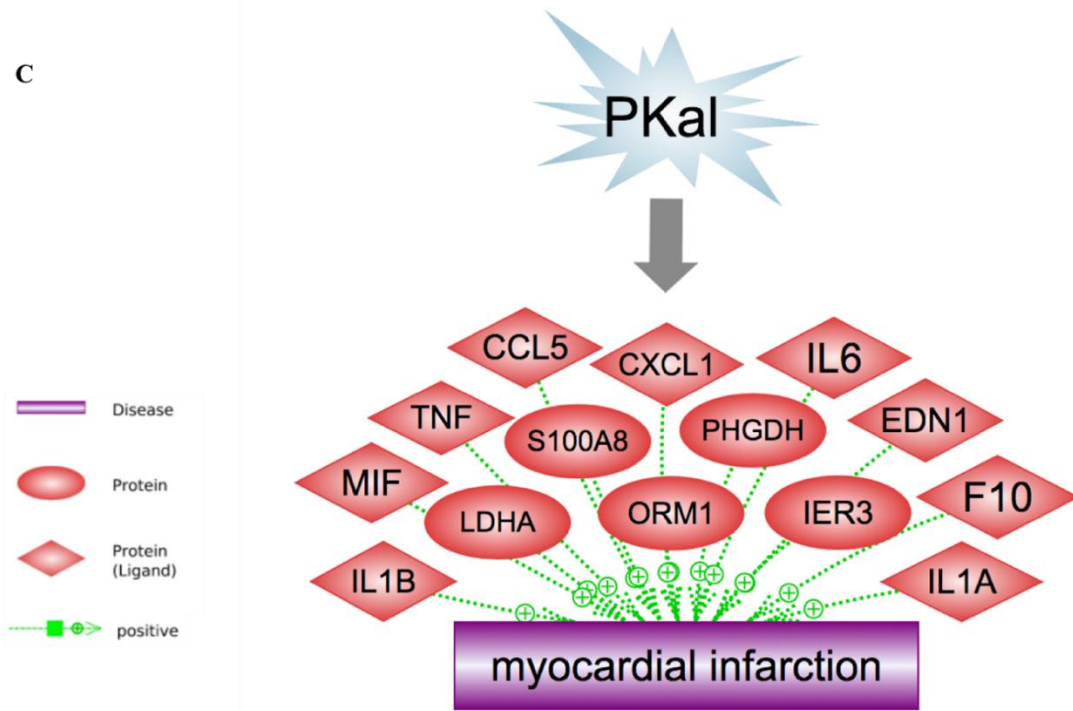
K. Network Pathway Analysis of Transcriptomic Data

Following RNA-sequencing analysis, the transcriptomic data was complemented with a stringent bioinformatics analysis using Elsevier's Pathway Studio software. This was performed in order to assess for pathway and protein interaction enrichment analysis, linking expressed proteins to cell processes and diseases. The program builds interactions within proteins and cellular states, with symbols on the arrows representing the type of interaction, according to the number of publications in the software's knowledge-base supporting this link. Fig. 24, Fig. 25 and Fig. 26 demonstrate the constructed pathways for individual treated groups.

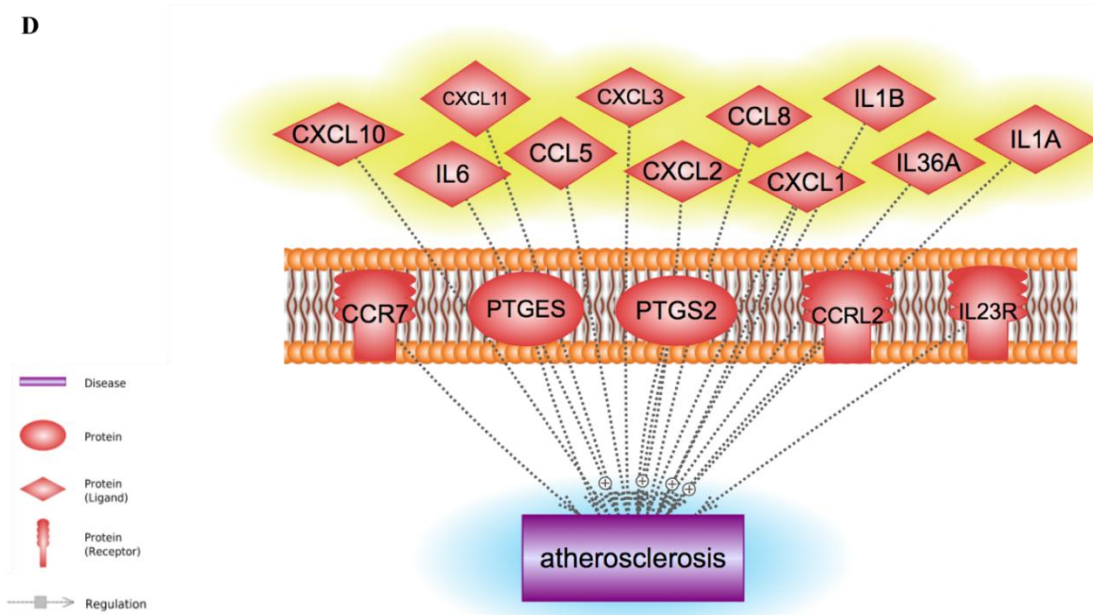




C



D



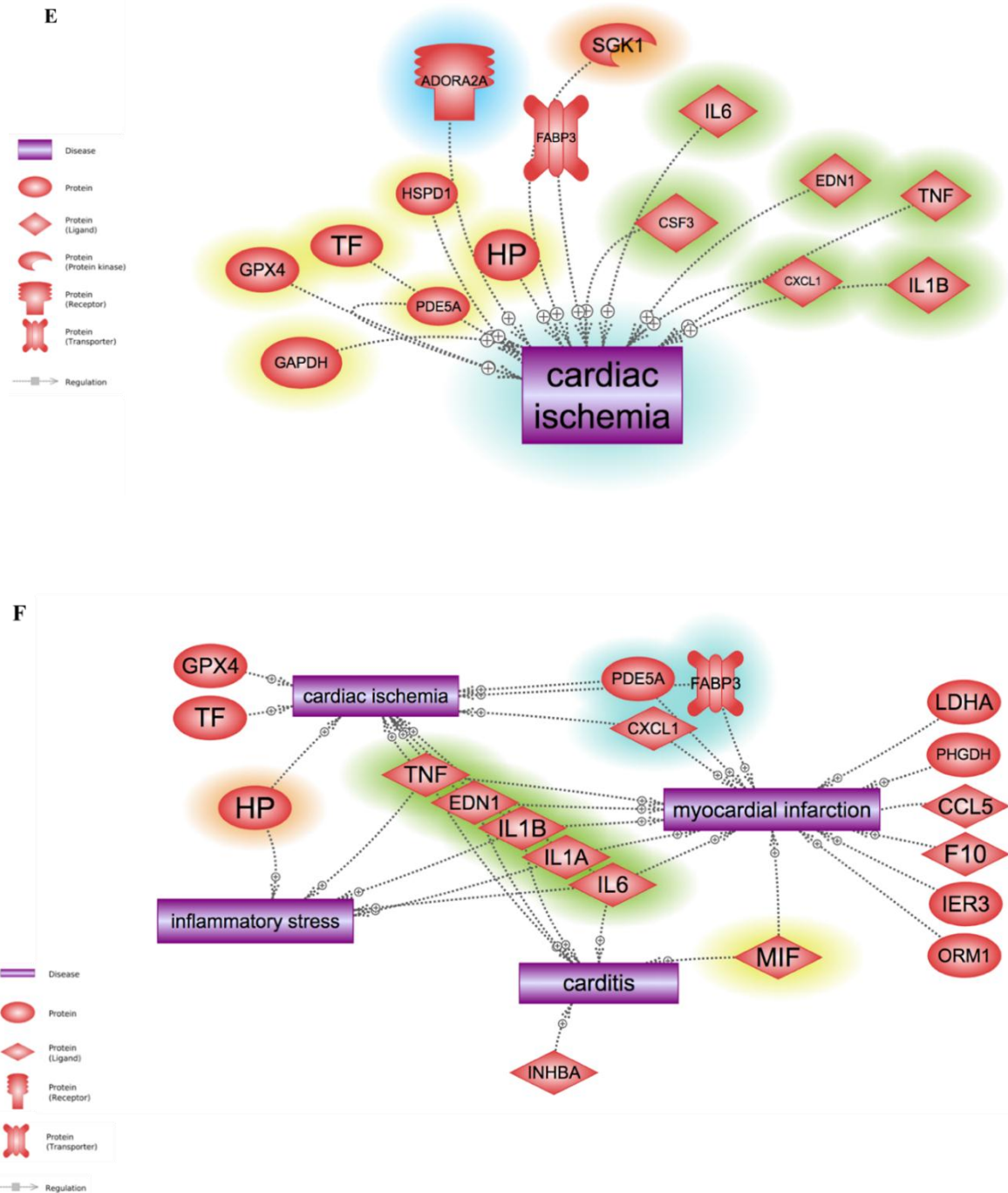
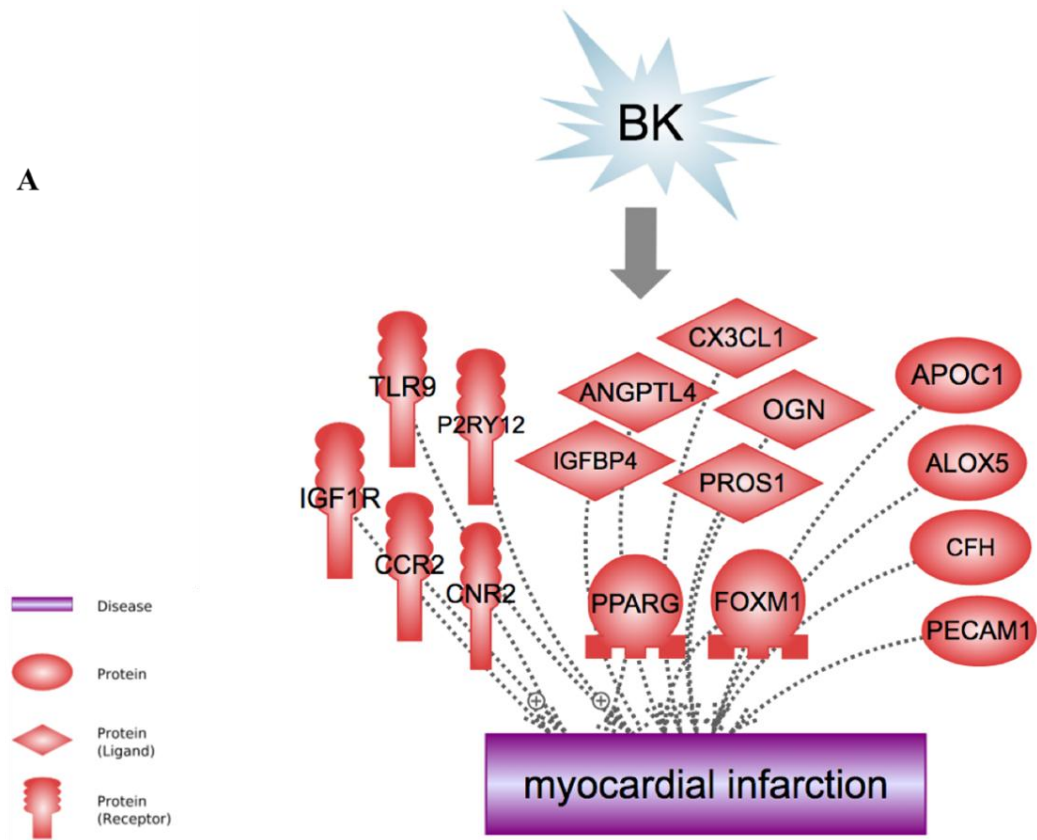


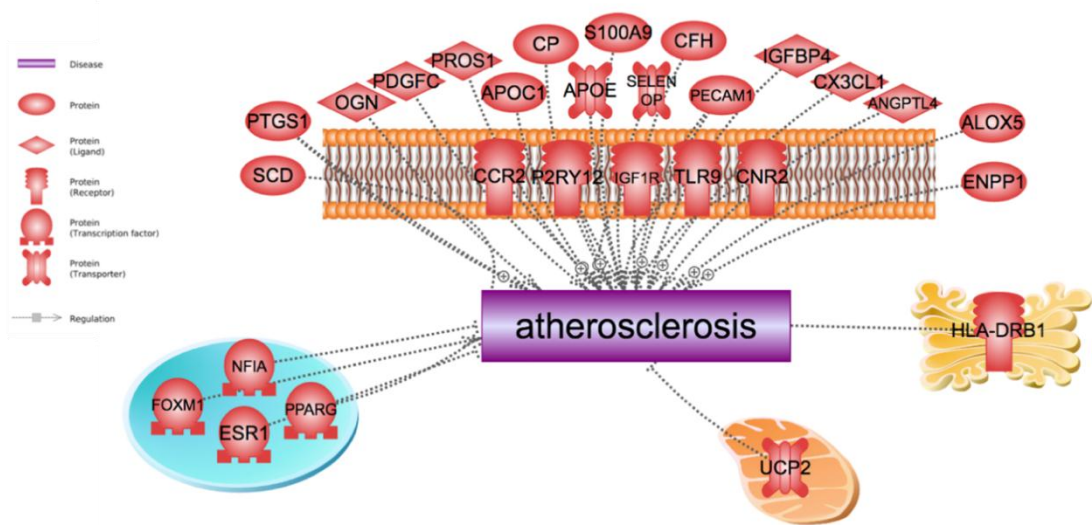
Figure 25 | Pathway Studio pathways relating expressed proteins in PK-stimulated macrophages to distinct proteins, cell processes and diseases. (A) Expressed proteins involved in the processes performed by M1 macrophages after stimulation with PK. **(B)** Common proteins expressed by macrophages involved in inflammation and myocardial infarction in response to PK. **(C)** Up-regulated and secreted proteins by macrophages

associated with and related to myocardial infarction. **(D)** Cytokines and chemokines secreted by macrophages involved in atherosclerosis. **(E)** Positive regulation of different proteins associated with cardiac ischemia. **(F)** Distinct proteins highly expressed in macrophages related to different diseases.

A



B



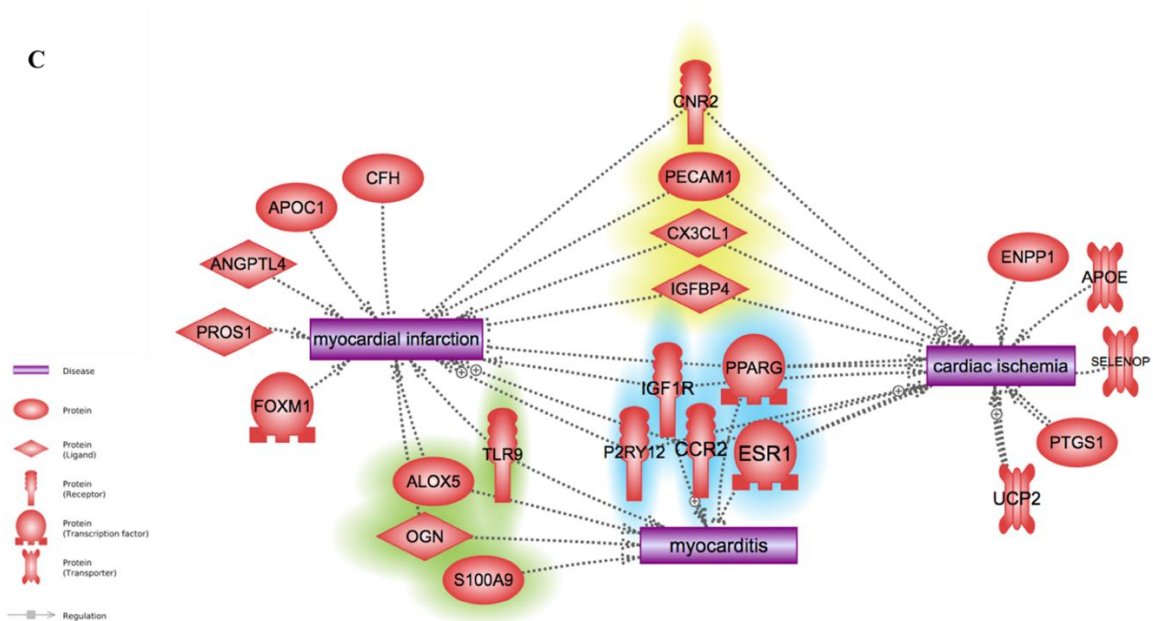


Figure 26 | Pathway Studio pathways relating expressed proteins in BK-stimulated macrophages to distinct proteins and diseases. (A) Up-regulated and secreted proteins by macrophages associated with and related to myocardial infarction. (B) Proteins expressed and secreted by macrophages involved in atherosclerosis. (C) Distinct proteins highly expressed in macrophages related to different diseases.

L. Investigation of Bradykinin and Protease-Activated Receptors Expression in Bone Marrow-Derived Macrophages

To assess the expression levels of bradykinin-1 and bradykinin-2 receptors as well as PAR-1 and PAR-2 receptors, RT-qPCR was performed on BMDM-extracted RNA. Figure 27 shows the relative expression of Bradykinin receptors as well as PAR receptors in untreated BMDM cells cultured for 24 hours.

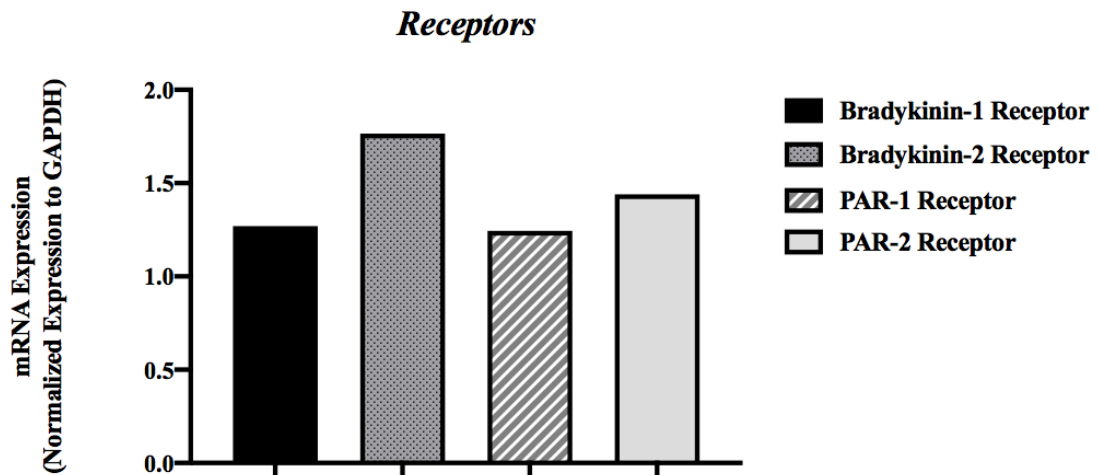


Figure 27 | Relative expression of four receptor genes in bone marrow-derived macrophages. Data is represented as mean (n=2).

M. Identification of Receptors in PK-Mediated Inflammatory Response

To further assess whether PK mediates its pro-inflammatory effect directly *via* activation of PARs, bone marrow-derived macrophages were stimulated with PK after in the presence and absence of PAR-1 (0.5 μ M) and PAR-2 (2 μ M) antagonists. PAR-1 and PAR-2 antagonists were added to BMDMs half an hour prior to PK-stimulation. Fig. 28 shows significant down-regulation of IL-6 and TNF- α expression by BMDMs in response to PAR-antagonists treatment as compared to PK-treatment alone.

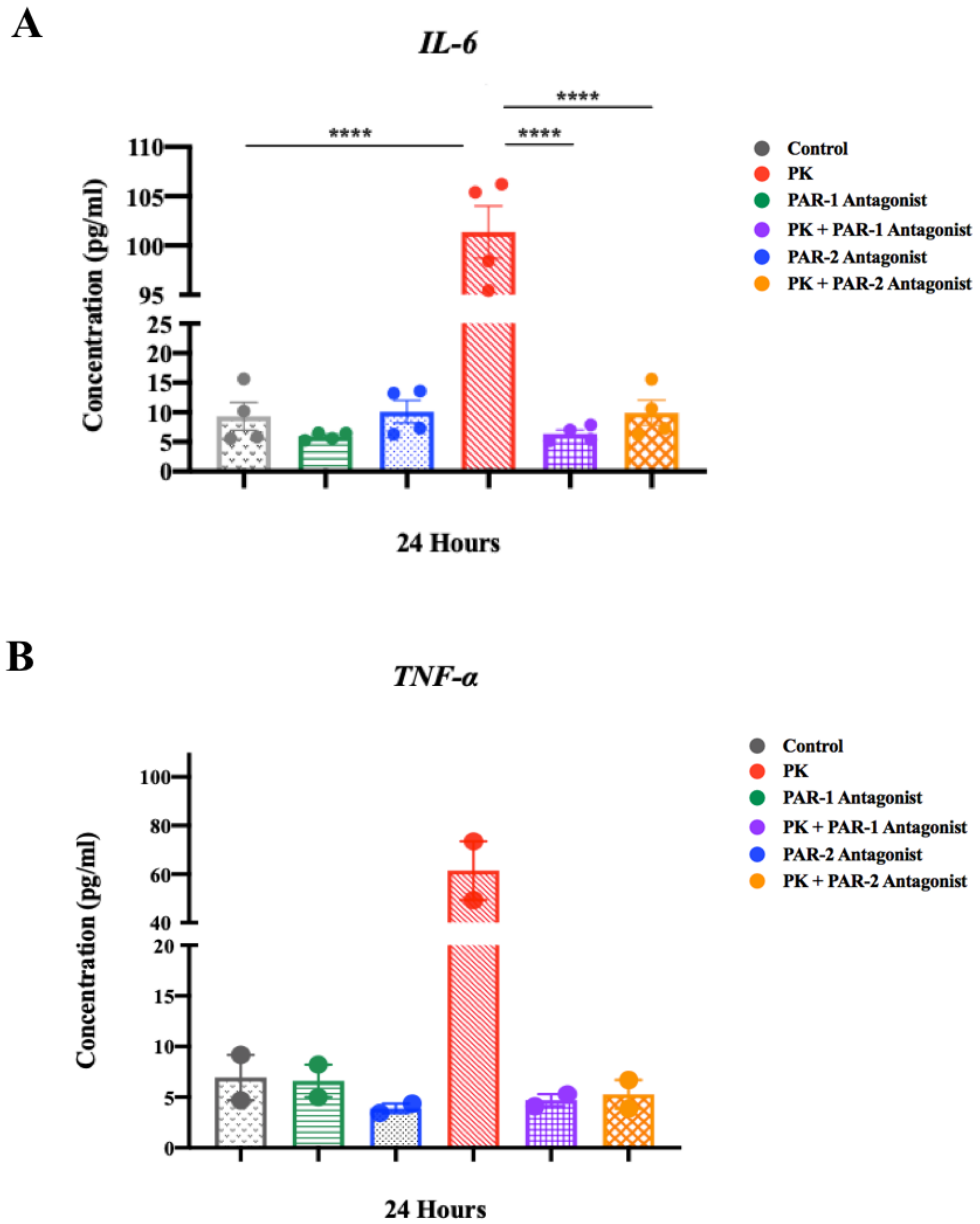


Figure 28 | IL-6 and TNF- α secretion by BMDMs after inhibiting PAR receptors. (A) IL-6 and **(B)** TNF- α secretion by BMDM cells. Data is represented as **(A)** mean \pm SEM (n=4), ****P < 0.0001 compared to the untreated control (Student's t-test) and **(B)** mean \pm SEM.

CHAPTER IV

DISCUSSION

Chronic inflammation is central to the development and pathogenesis of CVDs; particularly MI, whereby both innate and adaptive immune cells are involved in all phases of the disease. Earlier studies have shown that elevation of PK (the kininogenase of KKS) levels is implicated in the perpetuation of CVDs (Govers-Riemslog, Smid et al. 2007). In the current study, we investigated the mechanism through which PK and its downstream peptide, BK, can contribute to the pathogenesis of CVDs. Using murine bone marrow-derived macrophages, we first demonstrated the pro-inflammatory action of BK and PK through their positive effect on the secretion of IL-6 and TNF- α , renowned as pro-inflammatory cytokines. LPS, the lipopolysaccharide of the gram-negative bacterial cell wall, is known to induce systemic inflammation and thus was used as a positive control in our study. We next sought to elucidate gene expression signatures of BMDMs in response to BK and PK, in order to demarcate differentially expressed genes and profiles in the course of PK- and BK-mediated inflammatory processes using specific bioinformatics tools. This was done by RNA-sequencing using the NextSeq 550 Illumina platform. The variance among our different samples was verified using the DESeq2 tool on Galaxy based on the overall gene expression, which clearly indicated how distinct the different samples are. Our results have shown that PK has a different expression profile than the three other samples; control, LPS and BK. We then investigated the transcriptomic data generated from sequencing. After applying a Log₂ fold change of ± 1 and a p-adjusted < 0.05 , we

obtained around a thousand of different up- or down-regulated genes. Thereafter, we selected a set of known inflammatory, fibrotic, as well as oxidative stress genes so as to relate to our interest in PK- and BK-inflammatory-regulated processes (Table 4 and Table 5). Subsequently, we validated the expression of the aforementioned genes by RT-qPCR which confirmed the regulation of inflammatory genes; namely; IL-6, IL-1 β , TNF- α , MMP-9, CCL-2, and iNOS, with LPS-, BK-, and PK-treatments. Furthermore, we showed the shared up-regulated genes present in the different experimental groups by Venn diagrams upon adjustment of the Log₂ fold change to ± 2 for a greater stringency. Whereas 465 up-regulated genes were identified between LPS- and BK-treated samples, only 2 genes were common between LPS- and PK-treated samples as well as between BK- and PK-treated ones. Hence, the results from the Venn diagrams emphasize on the various inflammatory mechanisms induced by PK, which greatly differ from the ones activated by BK. This suggests that PK is most likely acting through mediators different than the known BK-signaling pathway. Although previous studies have shown that proteins implicated in the plasma KKS, such as BK, are related to inflammation (Motta and Tersariol 2017), our results suggest that PK is also capable of producing inflammation on its own, independent of its component, BK. Although the up-regulated genes were different among LPS-, BK-, and PK-treated samples, they all relate to inflammation in a way or another. In addition, the extent of up- or down-regulation was sometimes dissimilar for the same gene among the different samples. This denotes that there might be several pathways that could be mediated by the different players (LPS, BK, and PK) leading to inflammation. Accordingly, we constructed pathways using Elsevier's Pathway Studio software to evaluate protein-protein interactions and link expressed proteins to cell processes and diseases. Based on the genes

that were uploaded to the software, our data revealed the ability of PK to induce M1 macrophage phenotype just like LPS (Orekhov 2019), demonstrating the potency of PK to drive inflammation. This is clearly implied from its tendency to signal through the canonical NF- κ B pathway; which is known to control the transcription of cytokines, chemokines, and enzymatic genes of phagocytes, which are key players of acute inflammation (Tak and Firestein 2001). Moreover, although not significantly, our RT-qPCR data (Figure 23) has confirmed that PK can down-regulate the expression of MMP-9, while significantly up-regulate IL-6, TNF- α and iNOS favoring the polarization towards a classical macrophage phenotype. To our knowledge, this is the first study to demonstrate the direct role of PK in acute inflammation, and specifically in macrophage polarization. In addition, our data suggests the integral role of PK in CVDs, particularly in MI, atherosclerosis, cardiac ischemia, and carditis. This is supported by previous studies performed by Jaffa et al, designating PK as a marker of MI in diabetic patients (HUNT, JAFFA et al. 2019). Numerous studies support the detrimental role of different subsets of macrophages in dictating the fate of the injured myocardium; that is, regeneration versus fibrosis (Zlatanova, Pinto et al. 2016). Our results suggest that PK can perpetuate and exacerbate inflammation and thus aggravate cardiac remodeling in the context of MI by favoring the polarization of classical macrophages. On the other hand, our data also places BK as an essential factor involved in the same CVDs, although through different pathways and mediators. However, additional investigation is required to further characterize the detailed functional mode of PK in the previously mentioned diseases. Knowing that PK can act either directly through PARs (as shown in VSMCs) or indirectly through its downstream component, BK (Motta and Tersariol 2017), we verified the expression of

PAR and BK receptors in BMDM. Thus, to identify the receptor mediating PK-induced inflammation, we inhibited PARs 1/2 and stimulated the cells with PK. Our results show significant down-regulation of IL-6 and TNF- α secretion by BMDM upon treatment with both receptor antagonists, which firmly proves the notion that PK is acting *via* PARs. In conclusion, our data demonstrates for the first time that PK has a pro-inflammatory effect on macrophages, importantly through enhancing the classical macrophage polarization. By promoting inflammation, PK can have a vital role in different cardiovascular pathologies, which are evidently distinct from BK-dependent pathways. Although our studies need to be replicated on MI animal models to further investigate the interplay between PK and macrophages, as well as the exact mechanisms whereby PK contributes to cardiac remodeling, these results provide definitive evidence on the role of PK in inflammation and specifically its associative role in MI. Altogether, these findings pave the way for new therapeutic approaches.

REFERENCES

- Abdallah, R. T., J. S. Keum, et al. (2010). "Plasma kallikrein promotes epidermal growth factor receptor transactivation and signaling in vascular smooth muscle through direct activation of protease-activated receptors." J Biol Chem **285**(45): 35206-35215.
- Abdulaal, M., N. M. Haddad, et al. (2016). "The Role of Plasma Kallikrein-Kinin Pathway in the Development of Diabetic Retinopathy: Pathophysiology and Therapeutic Approaches." Semin Ophthalmol **31**(1-2): 19-24.
- Alan J. Mouton, O. J. R., Merry L. Lindsey (2018). "Myocardial infarction remodeling that progresses to heart failure: a signaling misunderstanding." American Journal of Physiology.
- An, L., S. An, et al. (2019). "Atorvastatin improves left ventricular remodeling and cardiac function in rats with congestive heart failure by inhibiting RhoA/Rho kinase-mediated endothelial nitric oxide synthase." Exp Ther Med **17**(1): 960-966.
- Anand, S. S., S. Islam, et al. (2008). "Risk factors for myocardial infarction in women and men: insights from the INTERHEART study." Eur Heart J **29**(7): 932-940.
- Bahou, W. F., W. C. Nierman, et al. (1993). "Chromosomal assignment of the human thrombin receptor gene: localization to region q13 of chromosome 5." Blood **82**(5): 1532-1537.
- Bates, S. M. and J. I. Weitz (2005). "Coagulation assays." Circulation **112**(4): e53-60.
- Beaubien, G., I. Rosinski-Chupin, et al. (1991). "Gene structure and chromosomal localization of plasma kallikrein." Biochemistry **30**(6): 1628-1635.
- Berg, D. D., S. D. Wiviott, et al. (2018). "Modes and timing of death in 66 252 patients with non-ST-segment elevation acute coronary syndromes enrolled in 14 TIMI trials." Eur Heart J **39**(42): 3810-3820.
- Bettelli, E., Y. Carrier, et al. (2006). "Reciprocal developmental pathways for the generation of pathogenic effector TH17 and regulatory T cells." Nature **441**(7090): 235-238.
- Bhatnagar, P., K. Wickramasinghe, et al. (2015). "The epidemiology of cardiovascular disease in the UK 2014." Heart **101**(15): 1182-1189.
- Biglu, M. H., M. Ghavami, et al. (2016). "Cardiovascular diseases in the mirror of science." J Cardiovasc Thorac Res **8**(4): 158-163.

- Binder, F., M. Hayakawa, et al. (2013). "Interleukin-4-induced β -catenin regulates the conversion of macrophages to multinucleated giant cells." Mol Immunol **54**(2): 157-163.
- Bjorkqvist, J., A. Jamsa, et al. (2013). "Plasma kallikrein: the bradykinin-producing enzyme." Thromb Haemost **110**(3): 399-407.
- Bryant, J. W. and Z. Shariat-Madar (2009). "Human plasma kallikrein-kinin system: physiological and biochemical parameters." Cardiovasc Hematol Agents Med Chem **7**(3): 234-250.
- Chen, L., H. Deng, et al. (2018). "Inflammatory responses and inflammation-associated diseases in organs." Oncotarget **9**(6): 7204-7218.
- Chistiakov, D. A., Y. V. Bobryshev, et al. (2015). "Macrophage phenotypic plasticity in atherosclerosis: The associated features and the peculiarities of the expression of inflammatory genes." Int J Cardiol **184**: 436-445.
- Christia, P., M. Bujak, et al. (2013). "Systematic characterization of myocardial inflammation, repair, and remodeling in a mouse model of reperfused myocardial infarction." J Histochem Cytochem **61**(8): 555-570.
- Clark, H. (2013). "NCDs: a challenge to sustainable human development." Lancet **381**(9866): 510-511.
- Clermont, A., Q. Zhou, et al. (2013). "Plasma Kallikrein Deficiency is protective against diabetes induced retinal vascular dysfunction." Invest Ophthalmol Vis Sci **54**(15): 1137-1137.
- Cochrane, C. G. and J. H. Griffin (1979). "Molecular assembly in the contact phase of the Hageman factor system." Am J Med **67**(4): 657-664.
- Cowie, M. R. (2017). "The heart failure epidemic: a UK perspective." Echo Res Pract **4**(1): R15-R20.
- Das, A., M. Sinha, et al. (2015). "Monocyte and macrophage plasticity in tissue repair and regeneration." Am J Pathol **185**(10): 2596-2606.
- Dutta, P. and M. Nahrendorf (2015). "Monocytes in myocardial infarction." Arterioscler Thromb Vasc Biol **35**(5): 1066-1070.
- Feener, E. P., Q. Zhou, et al. (2013). "Role of plasma kallikrein in diabetes and metabolism." Thromb Haemost **110**(3): 434-441.

- Ferrante, C. J., G. Pinhal-Enfield, et al. (2013). "The adenosine-dependent angiogenic switch of macrophages to an M2-like phenotype is independent of interleukin-4 receptor alpha (IL-4Ralpha) signaling." Inflammation **36**(4): 921-931.
- Fountoulaki, K., N. Dargès, et al. (2015). "Cellular Communications in the Heart." Card Fail Rev **1**(2): 64-68.
- Frangogiannis, N. G. (2006). "The mechanistic basis of infarct healing." Antioxid Redox Signal **8**(11-12): 1907-1939.
- Frangogiannis, N. G. (2008). "The immune system and cardiac repair." Pharmacol Res **58**(2): 88-111.
- Frangogiannis, N. G. (2015). "Inflammation in cardiac injury, repair and regeneration." Curr Opin Cardiol **30**(3): 240-245.
- G, M. P., V. R, et al. (1982). "Contact phase of blood coagulation in diabetes mellitus." European Journal of Clinical Investigation **12**(4): 307-311.
- Goldstein, J. A., D. Demetriou, et al. (2000). "Multiple complex coronary plaques in patients with acute myocardial infarction." N Engl J Med **343**(13): 915-922.
- Gombozhapova, A., Y. Rogovskaya, et al. (2017). "Macrophage activation and polarization in post-infarction cardiac remodeling." J Biomed Sci **24**(1): 13.
- Govers-Riemslog, J. W., M. Smid, et al. (2007). "The plasma kallikrein-kinin system and risk of cardiovascular disease in men." J Thromb Haemost **5**(9): 1896-1903.
- Gratchev, A., P. Guillot, et al. (2001). "Alternatively activated macrophages differentially express fibronectin and its splice variants and the extracellular matrix protein betaIG-H3." Scand J Immunol **53**(4): 386-392.
- Greaves, D. R. and K. M. Channon (2002). "Inflammation and immune responses in atherosclerosis." Trends Immunol **23**(11): 535-541.
- Haig, C., D. Carrick, et al. (2019). "Current Smoking and Prognosis After Acute ST-Segment Elevation Myocardial Infarction: New Pathophysiological Insights." JACC Cardiovasc Imaging **12**(6): 993-1003.
- Hamilton, J. A. (2008). "Colony-stimulating factors in inflammation and autoimmunity." Nat Rev Immunol **8**(7): 533-544.
- Hart, P. H., D. R. Burgess, et al. (1989). "Interleukin-4 stimulates human monocytes to produce tissue-type plasminogen activator." Blood **74**(4): 1222-1225.

- Heidt, T., G. Courties, et al. (2014). "Differential contribution of monocytes to heart macrophages in steady-state and after myocardial infarction." Circ Res **115**(2): 284-295.
- Herwald, H., T. Renne, et al. (1996). "Mapping of the discontinuous kininogen binding site of prekallikrein. A distal binding segment is located in the heavy chain domain A4." J Biol Chem **271**(22): 13061-13067.
- Heuberger, D. M. and R. A. Schuepbach (2019). "Protease-activated receptors (PARs): mechanisms of action and potential therapeutic modulators in PAR-driven inflammatory diseases." Thrombosis Journal **17**(1): 4.
- Hock, J., R. Vogel, et al. (1990). "High molecular weight kininogen-binding site of prekallikrein probed by monoclonal antibodies." J Biol Chem **265**(20): 12005-12011.
- HUNT, K. J., M. A. JAFFA, et al. (2019). "455-P: Levels of Plasma Prekallikrein Predict Myocardial Infarction in Non-Hispanic White Participants of the Veterans Affairs Diabetes Trial (VADT)." Diabetes **68**(Supplement 1): 455-P.
- Ibanez, B., S. James, et al. (2018). "2017 ESC Guidelines for the management of acute myocardial infarction in patients presenting with ST-segment elevation: The Task Force for the management of acute myocardial infarction in patients presenting with ST-segment elevation of the European Society of Cardiology (ESC)." Eur Heart J **39**(2): 119-177.
- Isailovic, N., K. Daigo, et al. (2015). "Interleukin-17 and innate immunity in infections and chronic inflammation." J Autoimmun **60**: 1-11.
- Isomi, M., T. Sadahiro, et al. (2019). "Progress and Challenge of Cardiac Regeneration to Treat Heart Failure." J Cardiol **73**(2): 97-101.
- Italiani, P. and D. Boraschi (2014). "From Monocytes to M1/M2 Macrophages: Phenotypical vs. Functional Differentiation." Front Immunol **5**: 514.
- Jaffa, M. A., D. Luttrell, et al. (2016). "Plasma Prekallikrein Is Associated With Carotid Intima-Media Thickness in Type 1 Diabetes." Diabetes **65**(2): 498-502.
- Jan., K. F. A. (2019). "Beta Blockers." StatPearls.
- Jenkins, S. J., D. Ruckerl, et al. (2011). "Local macrophage proliferation, rather than recruitment from the blood, is a signature of TH2 inflammation." Science **332**(6035): 1284-1288.
- Ji, R. R., Z. Z. Xu, et al. (2011). "Emerging roles of resolvins in the resolution of inflammation and pain." Trends Neurosci **34**(11): 599-609.

- Jung, K., P. Kim, et al. (2013). "Endoscopic time-lapse imaging of immune cells in infarcted mouse hearts." Circ Res **112**(6): 891-899.
- Jung, M., Y. Ma, et al. (2017). "IL-10 improves cardiac remodeling after myocardial infarction by stimulating M2 macrophage polarization and fibroblast activation." Basic Res Cardiol **112**(3): 33.
- Kahn, M. L., Y. W. Zheng, et al. (1998). "A dual thrombin receptor system for platelet activation." Nature **394**(6694): 690-694.
- Karin, M. and H. Clevers (2016). "Reparative inflammation takes charge of tissue regeneration." Nature **529**(7586): 307-315.
- Keum, J. S., M. A. Jaffa, et al. (2014). "Novel mechanism of plasma prekallikrein (PK) activation by vascular smooth muscle cells: evidence of the presence of PK activator." J Biol Regul Homeost Agents **28**(4): 587-603.
- Kolte, D., Shariat-Madar, Zia (2016). "Plasma Kallikrein Inhibitors in Cardiovascular Disease: An Innovative Therapeutic Approach." Cardiology in Review.
- Lauer, M., J. Kiley, et al. (2015). "National Heart, Lung, and Blood Institute (NHLBI) strategic visioning: setting an agenda together for the NHLBI of 2025." Journal of the American College of Cardiology **65**.
- Leuschner, F., P. Dutta, et al. (2011). "Therapeutic siRNA silencing in inflammatory monocytes in mice." Nat Biotechnol **29**(11): 1005-1010.
- Mantovani, A., A. Sica, et al. (2004). "The chemokine system in diverse forms of macrophage activation and polarization." Trends Immunol **25**(12): 677-686.
- Mantovani, A., S. Sozzani, et al. (2002). "Macrophage polarization: tumor-associated macrophages as a paradigm for polarized M2 mononuclear phagocytes." Trends Immunol **23**(11): 549-555.
- Maurer, M., M. Bader, et al. (2011). "New topics in bradykinin research." Allergy **66**(11): 1397-1406.
- Mechanic OJ, G. S. (2019). "Acute Myocardial Infarction." StatPearls Publishing.
- Mogensen, T. H. (2009). "Pathogen recognition and inflammatory signaling in innate immune defenses." Clin Microbiol Rev **22**(2): 240-273, Table of Contents.
- Mosser, D. M. and J. P. Edwards (2008). "Exploring the full spectrum of macrophage activation." Nat Rev Immunol **8**(12): 958-969.

- Motta, G. and I. L. S. Tersariol (2017). "Modulation of the Plasma Kallikrein-Kinin System Proteins Performed by Heparan Sulfate Proteoglycans." Frontiers in Physiology **8**(481).
- Nahrendorf, M. and F. K. Swirski (2013). "Monocyte and macrophage heterogeneity in the heart." Circ Res **112**(12): 1624-1633.
- Nahrendorf, M., F. K. Swirski, et al. (2007). "The healing myocardium sequentially mobilizes two monocyte subsets with divergent and complementary functions." J Exp Med **204**(12): 3037-3047.
- Nathan, C. and A. Ding (2010). "Nonresolving inflammation." Cell **140**(6): 871-882.
- Nich, C. and S. B. Goodman (2014). "Role of macrophages in the biological reaction to wear debris from joint replacements." J Long Term Eff Med Implants **24**(4): 259-265.
- Nichols, M., N. Townsend, et al. (2014). "Cardiovascular disease in Europe 2014: epidemiological update." Eur Heart J **35**(42): 2950-2959.
- Nystedt, S., K. Emilsson, et al. (1994). "Molecular cloning of a potential proteinase activated receptor." Proc Natl Acad Sci U S A **91**(20): 9208-9212.
- O'Rourke, S. A., A. Dunne, et al. (2019). "The Role of Macrophages in the Infarcted Myocardium: Orchestrators of ECM Remodeling." Frontiers in Cardiovascular Medicine **6**(101).
- Oishi, Y. and I. Manabe (2016). "Macrophages in age-related chronic inflammatory diseases." NPJ Aging Mech Dis **2**: 16018.
- Opie, L. H., P. J. Commerford, et al. (2006). "Controversies in ventricular remodelling." Lancet **367**(9507): 356-367.
- Orekhov, A. N. (2019). "Monocyte differentiation and macrophage polarization." Vessel Plus.
- Patrono, C., J. Morais, et al. (2017). "Antiplatelet Agents for the Treatment and Prevention of Coronary Atherothrombosis." J Am Coll Cardiol **70**(14): 1760-1776.
- Perbellini, F., S. A. Watson, et al. (2018). "Heterocellularity and Cellular Cross-Talk in the Cardiovascular System." Frontiers in Cardiovascular Medicine **5**(143).
- Pereira, R. L., R. J. Felizardo, et al. (2014). "Balance between the two kinin receptors in the progression of experimental focal and segmental glomerulosclerosis in mice." Dis Model Mech **7**(6): 701-710.

- Pesce, J. T., T. R. Ramalingam, et al. (2009). "Arginase-1-expressing macrophages suppress Th2 cytokine-driven inflammation and fibrosis." PLoS Pathog **5**(4): e1000371.
- Piepoli, M. F., A. W. Hoes, et al. (2016). "2016 European Guidelines on cardiovascular disease prevention in clinical practice: The Sixth Joint Task Force of the European Society of Cardiology and Other Societies on Cardiovascular Disease Prevention in Clinical Practice (constituted by representatives of 10 societies and by invited experts)Developed with the special contribution of the European Association for Cardiovascular Prevention & Rehabilitation (EACPR)." Eur Heart J **37**(29): 2315-2381.
- Porcu, P., C. Emanuelli, et al. (2004). "Circulating tissue kallikrein levels correlate with severity of carotid atherosclerosis." Arterioscler Thromb Vasc Biol **24**(6): 1104-1110.
- Randolph, G. J. (2009). "The fate of monocytes in atherosclerosis." J Thromb Haemost **7 Suppl 1**(Suppl 1): 28-30.
- Roffi, M., C. Patrono, et al. (2016). "2015 ESC Guidelines for the management of acute coronary syndromes in patients presenting without persistent ST-segment elevation: Task Force for the Management of Acute Coronary Syndromes in Patients Presenting without Persistent ST-Segment Elevation of the European Society of Cardiology (ESC)." Eur Heart J **37**(3): 267-315.
- Russo, A., U. Soh, et al. (2009). "Proteases Display Biased Agonism at Protease-Activated Receptors: Location Matters!" Molecular interventions **9**: 87-96.
- Sansbury, B. E. and M. Spite (2016). "Resolution of Acute Inflammation and the Role of Resolvins in Immunity, Thrombosis, and Vascular Biology." Circ Res **119**(1): 113-130.
- Schmidt, V. A., W. C. Nierman, et al. (1998). "The human proteinase-activated receptor-3 (PAR-3) gene. Identification within a Par gene cluster and characterization in vascular endothelial cells and platelets." J Biol Chem **273**(24): 15061-15068.
- Serhan, C. N., S. D. Brain, et al. (2007). "Resolution of inflammation: state of the art, definitions and terms." FASEB J **21**(2): 325-332.
- Shariat-Madar, Z., F. Mahdi, et al. (2002). "Identification and characterization of prolylcarboxypeptidase as an endothelial cell prekallikrein activator." J Biol Chem **277**(20): 17962-17969.
- Soh, U. J., M. R. Dores, et al. (2010). "Signal transduction by protease-activated receptors." Br J Pharmacol **160**(2): 191-203.

- Tak, P. P. and G. S. Firestein (2001). "NF-kappaB: a key role in inflammatory diseases." J Clin Invest **107**(1): 7-11.
- ter Horst, E. N., N. Hakimzadeh, et al. (2015). "Modulators of Macrophage Polarization Influence Healing of the Infarcted Myocardium." Int J Mol Sci **16**(12): 29583-29591.
- Thomas, P. D., M. J. Campbell, et al. (2003). "PANTHER: a library of protein families and subfamilies indexed by function." Genome Res **13**(9): 2129-2141.
- Tschope, C., P. Gohlke, et al. (1997). "Antihypertensive and cardioprotective effects after angiotensin-converting enzyme inhibition: role of kinins." J Card Fail **3**(2): 133-148.
- Tushinski, R. J., I. T. Oliver, et al. (1982). "Survival of mononuclear phagocytes depends on a lineage-specific growth factor that the differentiated cells selectively destroy." Cell **28**(1): 71-81.
- Urban J, S. A., Huber A, Lippman S, Mukhopadhyay D, Deloche O, Wanke V, Anrather D, Ammerer G, Riezman H (2007). "Sch9 is a major target of TORC1 in *Saccharomyces cerevisiae*." Mol Cell.
- van Furth, R. and Z. A. Cohn (1968). "The origin and kinetics of mononuclear phagocytes." J Exp Med **128**(3): 415-435.
- Varga, T., R. Mounier, et al. (2016). "Highly Dynamic Transcriptional Signature of Distinct Macrophage Subsets during Sterile Inflammation, Resolution, and Tissue Repair." J Immunol **196**(11): 4771-4782.
- Wang, B. X., W. Kit-Anan, et al. (2018). "Many Cells Make Life Work-Multicellularity in Stem Cell-Based Cardiac Disease Modelling." Int J Mol Sci **19**(11).
- Weintraub, W. S., S. R. Daniels, et al. (2011). "Value of primordial and primary prevention for cardiovascular disease: a policy statement from the American Heart Association." Circulation **124**(8): 967-990.
- Weiskopf, K., P. J. Schnorr, et al. (2016). "Myeloid Cell Origins, Differentiation, and Clinical Implications." Microbiol Spectr **4**(5).
- Wheeler, A. P. and D. Gailani (2016). "The Intrinsic Pathway of Coagulation as a Target for Antithrombotic Therapy." Hematol Oncol Clin North Am **30**(5): 1099-1114.
- (WHO), W. H. O. (n.d). "Cardiovascular diseases." Retrieved February 24, 2020, from https://www.who.int/health-topics/cardiovascular-diseases/#tab=tab_1.

- Wynn, T. A. (2008). "Cellular and molecular mechanisms of fibrosis." J Pathol **214**(2): 199-210.
- Yan, X., A. Anzai, et al. (2013). "Temporal dynamics of cardiac immune cell accumulation following acute myocardial infarction." J Mol Cell Cardiol **62**: 24-35.
- Yao, Y., X.-H. Xu, et al. (2019). "Macrophage Polarization in Physiological and Pathological Pregnancy." Front Immunol **10**(792).
- Yap, J., H. A. Cabrera-Fuentes, et al. (2019). "Role of Macrophages in Cardioprotection." Int J Mol Sci **20**(10).
- Yeh, R. W., S. Sidney, et al. (2010). "Population trends in the incidence and outcomes of acute myocardial infarction." N Engl J Med **362**(23): 2155-2165.
- Zhang, Q., M. Raouf, et al. (2010). "Circulating mitochondrial DAMPs cause inflammatory responses to injury." Nature **464**(7285): 104-107.
- Zlatanova, I., C. Pinto, et al. (2016). "Immune Modulation of Cardiac Repair and Regeneration: The Art of Mending Broken Hearts." Frontiers in Cardiovascular Medicine **3**(40).

